# Spacecraft Angular Velocity and Line-of-Sight Control Using A Single-Gimbal Variable-Speed Control Moment Gyro

Hyungjoo Yoon* and Panagiotis Tsiotras†
*Georgia Institute of Technology*
*Atlanta, Georgia 30332-0150, USA*

**It is well known that complete attitude control of a spacecraft is not possible with only one single-gimbal Variable-Speed Control Moment Gyro (VSCMG) due to the conservation of the angular momentum. However, partial attitude control without violating the angular momentum conservation principle is still possible. In this paper, feedback controllers that stabilize the angular velocity vector of a rigid spacecraft with additional partial attitude stabilization using a single VSCMG are presented. A pair of angles is chosen to parameterize all feasible final spacecraft orientations at rest. Based on this parametrization, an LQR control law is designed to locally stabilize the spacecraft angular velocity, while also controlling a given spacecraft body-axis in inertial space. A multi-stage control law is also suggested to achieve the same control objective in the large.**

## I. Introduction

Recent advances in spacecraft and satellite control systems have succeeded in solving several challenging problems dealing with the attitude tracking and control of rigid and flexible spacecraft, optimal slew maneuvers, precision pointing, formation flying, etc. Techniques from nonlinear, adaptive, optimal and robust control[1–11] have been used to his end with great success. Most–if not all–of these results have been developed under the assumption that the spacecraft is actively controlled with a sufficient number of actuators, which is equal to, or even larger than, the number of the degrees of freedom of the system. Although this is certainly the case with most current spacecraft, the issue of controlling a rigid spacecraft with less than three control torques has recently aroused the interest of many researchers, as it provides the theoretical foundation to account for unexpected actuator failures. It also allows the minimization of the required number of actuators to perform certain missions thus reducing weight and even cost.

Several papers have been published on the stabilization of the angular velocity (or detumbling) of a rigid spacecraft with less than three control torques.[12–16] In these works only the dynamic (or kinetic) equations are under consideration, and the objective is to null the angular velocity vector of the spacecraft. Stabilization of the much more difficult complete equations (dynamics and kinematics) has also been addressed;[17–23] the objective of these references is to stabilize a spacecraft about a desired reference attitude with less than three control torques. See Ref. 24 for a full survey of the underactuated spacecraft control literature up to that time. In all previous references, the control torques are assumed to be provided by some external mechanism (e.g., gas jets or magnetotorquers, etc). Alternatively, internal torques generated by momentum exchange devices, such as reaction or momentum wheels or control moment gyros (CMGs) can also be used for attitude control of a spacecraft. Only few researchers have worked on the attitude stabilization,[25,26] detumbling and/or angular velocity control[27–29] problem using less than three reaction wheels.

Recently, a new alternative for spacecraft attitude control has become available, namely that of a *variable-speed* control moment gyro (VSCMG). A VSCMG is a hybrid actuator which combines a reaction/momentum

*Currently with Samsung Electronics Co., Korea. Email: drake.yoon@gmail.com. Tel: +82-10-2313-1097. Student Member AIAA.

†Professor, School of Aerospace Engineering. Email: p.tsiotras@ae.gatech.edu. Tel: (404) 894-9526. Fax: (404) 894-2760. Associate Fellow AIAA. Corresponding author.

wheel (RW/MW) with a single-gimbal control moment gyro.[30–34] Whereas the wheel speed of a conventional CMG is kept constant, the wheel speed of a VSCMG is allowed to vary continuously. Therefore, while a RW/MW or a conventional CMG can only generate a torque along a single direction at any instant of time, a VSCMG can generate a torque that lies anywhere on a plane perpendicular to the gimbal axis. Hence, a cluster of VSCMGs can generate a torque at an arbitrarily direction in the three dimensional space, as long as at least two or more VSCMGs are used, whose gimbal directions are not parallel to each other.[31] Moreover, the extra degree of freedom of a VSCMG can be used for additional purposes, for instance, for combined attitude and power tracking control[33] and/or singularity avoidance.[32,34]

Recently, Tsiotras et al. have addressed the stabilization of a spacecraft via a VSCMG actuator.[35] In Ref. 35, it is shown that complete attitude stabilization may not always be possible due to the angular momentum conservation constraint, but the angular velocity system is linearly controllable, hence stabilizable. Both linear LQR feedback controllers and a nonlinear controller were designed in Ref. 35 for stabilizing the angular velocity equations.

In the present paper, we provide some new results for the angular velocity stabilization of a spacecraft via a single VSCMG, while also achieving partial attitude control. Even though complete attitude control is impossible due to the momentum conservation constraint, it is still possible to achieve stabilization about certain orientations lying in a feasible orientation manifold. We investigate this possibility and provide both linear and nonlinear controllers which locally and semi-globally[a].

stabilize the angular velocity system. These controllers also regulate the spacecraft attitude so that a body-fixed axis aims at a given inertial direction. This problem is of interest not only from a theoretical point of view, but also from a practical point of view. For instance, if we install a camera or an antenna fixed on the spacecraft, then we can control the line-of-sight of this camera/antenna so that it points along a desired direction with a single VSCMG. Therefore, if for a specific mission one does not need to track the complete attitude, then a single VSCMG is sufficient to achieve this control objective. Moreover, our study also characterizes the types of missions that are possible when some of the VSCMG actuators used for the spacecraft attitude control accidentally fail.

The paper is organized as follows. In Section II, we provide the equations of motion of a spacecraft with one VSCMG actuator. We specialize the full dynamic equation of a spacecraft with a cluster of multiple VSCMGs of Ref. 33 to the case with a single VSCMG. In Section III all feasible spacecraft orientations, which do not violate the momentum conservation are investigated, and a parametrization of these feasible orientations is suggested. The control objective is subsequently formulated in terms of this parametrization. In Section IV, the system equations are linearized near the desired state, and the controllability issue is studied. An LQR feedback controller which locally achieves the control objective is proposed. A global controller that achieves the same control objective from all initial conditions is given in Section V. Finally, in Section VI we present numerical examples to verify the proposed control methodology.

## II. Equation of Motion

The dynamic equations of motion of a spacecraft with a cluster of VSCMGs have been fully derived in the literature.[30,31,33,36] Herein, we will use the equations as given by Yoon and Tsiotras.[33] In Ref. 33 the equations are derived under the assumptions that the center of mass of each VSCMG wheel coincides with that of the gimbal structure; the spacecraft, wheels, and gimbal structure are rigid; the flywheels and gimbals are balanced; and the spacecraft rotational motion is decoupled from its translational motion. Figure 1 shows a schematic of a spacecraft with a single VSCMG. The body-frame $\mathcal{B}$ is represented by the orthonormal set of unit vectors $\hat{\mathbf{b}}_1$, $\hat{\mathbf{b}}_2$ and $\hat{\mathbf{b}}_3$, and its origin is located at the center of mass of the entire spacecraft. The gimbal frame $\mathcal{G}$ is represented by the orthonormal set of unit vectors $\hat{\mathbf{s}}$, $\hat{\mathbf{t}}$ and $\hat{\mathbf{g}}$, and it is located on the gimbal, as shown in Fig. 1.

Specializing the dynamical equations of motion of Ref. 33 to the single VSCMG case, one obtains,

$$J\dot{\boldsymbol{\omega}} + \dot{J}\boldsymbol{\omega} + I_{\rm cg}\ddot{\gamma}\hat{\mathbf{g}} + I_{\rm ws}\Omega\dot{\gamma}\hat{\mathbf{t}} + I_{\rm ws}\dot{\Omega}\hat{\mathbf{s}} + \boldsymbol{\omega}^{\times}\mathbf{h} = 0, \tag{1}$$

where the total angular momentum vector $\mathbf{h}$ of the spacecraft is expressed in the $\mathcal{B}$-frame as

$$\mathbf{h} \triangleq J\boldsymbol{\omega} + I_{\rm cg}\dot{\gamma}\hat{\mathbf{g}} + I_{\rm ws}\Omega\hat{\mathbf{s}}. \tag{2}$$

[a]As usual, semi-global stability refers to the type of stability with respect to all initial conditions from an *a posteriori* arbitrarily large set; in contrast to global stability, the controller gains depend on the size of this set.

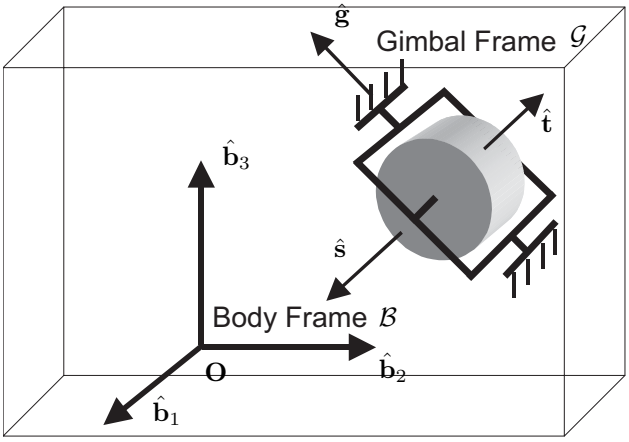


**Figure 1. Rigid spacecraft with a single VSCMG.**

Here $J$ is the inertia matrix of the whole spacecraft (including the VSCMG), $\Omega$ is the wheel spin rate of the VSCMG with respect to the spacecraft, $I_{\rm ws}$ is a moment of inertia of the wheel about its spin axis, and $I_{\rm cg}$ is the sum of the inertia of the wheel and gimbal structure about the gimbal axis. For any vector $\boldsymbol{v} = [v_1, v_2, v_3]^T \in \mathbb{R}^3$, the notation $\boldsymbol{v}^\times \in \mathbb{R}^{3\times 3}$ represents the equivalent vector cross product operation, that is,

$$\boldsymbol{v}^\times \triangleq \begin{bmatrix} 0 & -v_3 & v_2 \\ v_3 & 0 & -v_1 \\ -v_2 & v_1 & 0 \end{bmatrix}.$$

The total moment of inertia of the spacecraft will change, in general, as the VSCMG rotates about its gimbal axis, so the matrix $J = J(\gamma)$ is a function of a gimbal angle $\gamma$; see the second term in Eq. (1). However, the dependence of $J$ on $\gamma$ is weak, especially when the size of spacecraft main body is large. We will therefore assume that $J$ is constant ($\dot{J} = 0$) during controller design. In addition, to simplify the analysis, we assume that the gimbal acceleration term $I_{\rm cg}\ddot{\gamma}\hat{\mathbf{g}}$ is ignored. This assumption is standard in the literature,[30,31,33,36] and it amounts to gimbal angle rate servo control. Under these assumptions, the dynamic equation (1) can be simplified as

$$\begin{aligned} J\dot{\boldsymbol{\omega}} &= -\boldsymbol{\omega}^\times \mathbf{h} - I_{\rm ws}\Omega\dot{\gamma}\hat{\mathbf{t}} - I_{\rm ws}\dot{\Omega}\hat{\mathbf{s}} \\ &= -\boldsymbol{\omega}^\times (J\boldsymbol{\omega} + I_{\rm cg}\dot{\gamma}\hat{\mathbf{g}} + I_{\rm ws}\Omega\hat{\mathbf{s}}) - I_{\rm ws}\Omega\dot{\gamma}\hat{\mathbf{t}} - I_{\rm ws}\dot{\Omega}\hat{\mathbf{s}} \\ &= -\boldsymbol{\omega}^\times (J\boldsymbol{\omega} + I_{\rm cg}\dot{\gamma}\hat{\mathbf{g}} + I_{\rm ws}\Omega\hat{\mathbf{s}}) - I_{\rm ws}\Omega\hat{\mathbf{t}}u_1 - I_{\rm ws}\hat{\mathbf{s}}u_2, \end{aligned} \tag{3}$$

where the control input is

$$\mathbf{u} \triangleq \begin{bmatrix} u_1 \\ u_2 \end{bmatrix} = \begin{bmatrix} \dot{\gamma} \\ \dot{\Omega} \end{bmatrix}. \tag{4}$$

## III. Parametrization of the Spacecraft Orientations at Rest

Because the VSCMG is an internal momentum exchange actuator, the total angular momentum of the spacecraft is conserved (in both magnitude and direction) during a maneuver, assuming no external control/disturbance torques are applied to the spacecraft. Therefore, for a given nonzero initial total angular momentum vector $\mathbf{H}_0$, the final rest state of the spacecraft and the VSCMG is such that, the direction of the spin axis of the VSCMG is aligned with $\mathbf{H}_0$, and the magnitude of the angular momentum of the wheel is equal to the initial magnitude of the angular momentum vector $H_0 \triangleq \|\mathbf{H}_0\|$. That is,

$$\mathbf{H}_0 = I_{\rm ws}\Omega_{\rm f}\hat{\mathbf{s}}_{\rm f} = \operatorname{sgn}\Omega_{\rm f}\, H_0\, \hat{\mathbf{s}}_{\rm f} \tag{5}$$

where the subscript 'f' denotes the desired final state, when the spacecraft is at rest and $\operatorname{sgn}\Omega_f$ denotes the sign of $\Omega_f$. Since the final spin axis of the VSCMG is determined by the initial angular momentum $\mathbf{H}_0$, the spacecraft attitude at rest can be determined via only two rotations: one is a rotation of the spacecraft about the gimbal axis, and the other is a rotation of the spacecraft about the final spin axis. Since at least three parameters are needed to express the complete orientation of a spacecraft, one expects that complete attitude control of the spacecraft is not possible using one VSCMG; see Ref. 35 for a formal proof of this claim. As a result, the set of all feasible final spacecraft orientations at rest for a given initial angular momentum $\mathbf{H}_0$ can be parameterized by a pair of two angles.

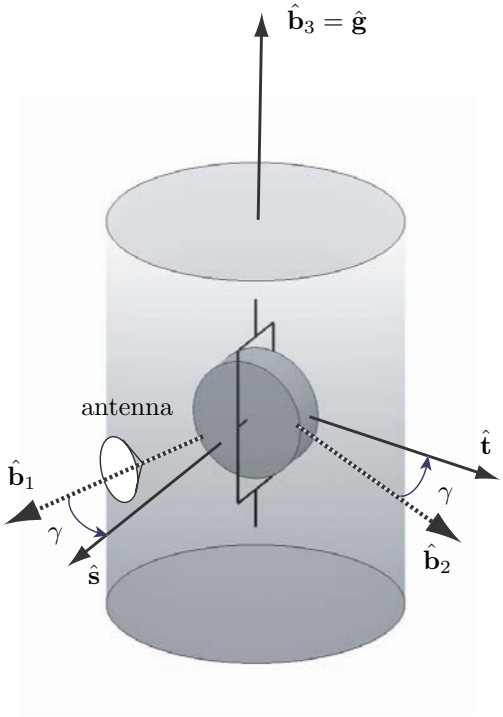


**Figure 2. Axes definition of a spacecraft with a VSCMG and an antenna.**

Note that the geometric constraint that the wheel spin axis is aligned with $\mathbf{H}_0$ implies that the gimbal axis must be perpendicular to $\mathbf{H}_0$, whenever the spacecraft is at rest. Therefore, if we install a camera or an antenna on the spacecraft so that its line-of-sight is fixed in the plane normal to the gimbal axis, we can aim the line-of-sight at any given inertial direction $\hat{\mathbf{n}}$. Before providing a formal proof of the last statement, we investigate all possible final orientations of the spacecraft when it comes to rest.

To this end, and without loss of generality, let us assume that the gimbal axis is fixed along the $\hat{\mathbf{b}}_3$-body axis, and the camera/antenna is fixed along the $\hat{\mathbf{b}}_1$-body axis, as shown in Fig. 2. The gimbal angle $\gamma$ is defined as the angle from $\hat{\mathbf{b}}_1$ to $\hat{\mathbf{s}}$ about the $\hat{\mathbf{g}} = \hat{\mathbf{b}}_3$ axis. The spin axis of the VSCMG can then be written as

$$\hat{\mathbf{s}} = \cos\gamma\, \hat{\mathbf{b}}_1 + \sin\gamma\, \hat{\mathbf{b}}_2. \tag{6}$$

We introduce the following parametrization of the spacecraft orientation. First, we define an inertial frame $\mathcal{H}$ with basis vectors $\hat{\mathbf{a}}_1, \hat{\mathbf{a}}_2, \hat{\mathbf{a}}_3$, so that the total angular momentum $\mathbf{H}_0$ is aligned along $\hat{\mathbf{a}}_3$, that is,

$$\hat{\mathbf{a}}_3 \triangleq \frac{\mathbf{H}_0}{H_0}. \tag{7}$$

Given an inertial direction $\hat{\mathbf{n}}$ (which is not parallel with $\mathbf{H}_0$), we define the remaining two unit vectors by

$$\hat{\mathbf{a}}_2 = \frac{\hat{\mathbf{a}}_3 \times \hat{\mathbf{n}}}{\|\hat{\mathbf{a}}_3 \times \hat{\mathbf{n}}\|}, \qquad \hat{\mathbf{a}}_1 = \hat{\mathbf{a}}_2 \times \hat{\mathbf{a}}_3. \tag{8}$$

When $\hat{\mathbf{n}}$ is parallel to $\mathbf{H}_0$, one may define $\hat{\mathbf{a}}_1$ and $\hat{\mathbf{a}}_2$ arbitrarily as two unit vectors normal to $\hat{\mathbf{n}}$, so that the three vectors of $\hat{\mathbf{a}}_1, \hat{\mathbf{a}}_2, \hat{\mathbf{a}}_3$ form an orthonormal set.

Any spacecraft orientation can be described by a "3-1-3" body-axis angel sequence from frame $\mathcal{H}$ to frame $\mathcal{B}$ via the direction cosine matrix $R_{\mathcal{H}}^{\mathcal{B}}$ from $\mathcal{H}$ to $\mathcal{B}$, defined as $R_{\mathcal{H}}^{\mathcal{B}} = R_3(\psi)R_1(\theta)R_3(\phi)$, where $R_i$, for $i = 1, 2, 3$ is the rotational matrix about the $i$th body-axis. Componentwise, we can write

$$R_{\mathcal{H}}^{\mathcal{B}} = \begin{bmatrix} \mathrm{c}\phi\,\mathrm{c}\psi - \mathrm{s}\phi\,\mathrm{c}\theta\,\mathrm{s}\psi & \mathrm{s}\phi\,\mathrm{c}\psi + \mathrm{c}\phi\,\mathrm{c}\theta\,\mathrm{s}\psi & \mathrm{s}\theta\,\mathrm{s}\psi \\ -\mathrm{c}\phi\,\mathrm{s}\psi - \mathrm{s}\phi\,\mathrm{c}\theta\,\mathrm{c}\psi & -\mathrm{s}\phi\,\mathrm{s}\psi + \mathrm{c}\phi\,\mathrm{c}\theta\,\mathrm{c}\psi & \mathrm{s}\theta\,\mathrm{c}\psi \\ \mathrm{s}\phi\,\mathrm{s}\theta & -\mathrm{c}\phi\,\mathrm{s}\theta & \mathrm{c}\theta \end{bmatrix}, \tag{9}$$

where $\theta \in [0, \pi]$, and $\phi, \psi \in (-\pi, \pi]$, and $\mathrm{c}\phi \triangleq \cos\phi$, $\mathrm{s}\phi \triangleq \sin\phi$, etc. From (5), (6) and (7), one now has

$$\operatorname{sgn}\Omega_{\mathrm{f}} \begin{bmatrix} \cos\gamma_{\mathrm{f}} \\ \sin\gamma_{\mathrm{f}} \\ 0 \end{bmatrix} = R_{\mathcal{H}}^{\mathcal{B}}\,\hat{\mathbf{a}}_3 = \begin{bmatrix} \sin\theta_{\mathrm{f}}\,\sin\psi_{\mathrm{f}} \\ \sin\theta_{\mathrm{f}}\,\cos\psi_{\mathrm{f}} \\ \cos\theta_{\mathrm{f}} \end{bmatrix}, \tag{10}$$

for the case when the spacecraft and the VSCMG gimbal are both at rest. Comparing the third element of (10) yields $\cos\theta_{\mathrm{f}} = 0$, i.e., $\theta_{\mathrm{f}} = \pi/2$. Physically, this implies that the only orientations which are accessible at rest are those for which the $\hat{\mathbf{b}}_3$-axis (the gimbal axis) is perpendicular to the total angular momentum. Therefore, all feasible spacecraft orientations at rest can be parameterized by the pair of the two Euler angles $\phi_{\mathrm{f}}$ and $\psi_{\mathrm{f}}$. Since $\theta_{\mathrm{f}} = \pi/2$ it follows that $\sin\theta_{\mathrm{f}} = 1$. Hence $\cos\gamma_{\mathrm{f}} = \operatorname{sgn}\Omega_{\mathrm{f}}\sin\psi_{\mathrm{f}}$, and $\sin\gamma_{\mathrm{f}} = \operatorname{sgn}\Omega_{\mathrm{f}}\cos\psi_{\mathrm{f}}$. This yields a relation between the final gimbal angle $\gamma_{\mathrm{f}}$ and the final Euler angle $\psi_{\mathrm{f}}$ as follows

$$\gamma_{\mathrm{f}} = \operatorname{sgn}\Omega_{\mathrm{f}}\,(\pi/2) - \psi_{\mathrm{f}}. \tag{11}$$

This means that the final Euler angle $\psi_{\mathrm{f}}$ at rest is determined by the final gimbal angle $\gamma_{\mathrm{f}}$ if the sign $\boldsymbol{\Omega}_{\mathrm{f}}$ is known. Therefore, we can use the gimbal angle $\gamma_{\mathrm{f}}$ as one of the parameters to describe the spacecraft orientation at rest, in lieu of $\psi_{\mathrm{f}}$. In the sequel, we denote $\gamma_{\mathrm{f}}^{+} = \pi/2 - \psi_{\mathrm{f}}$ and $\gamma_{\mathrm{f}}^{-} = -\pi/2 - \psi_{\mathrm{f}} = \gamma_{\mathrm{f}}^{+} - \pi$.

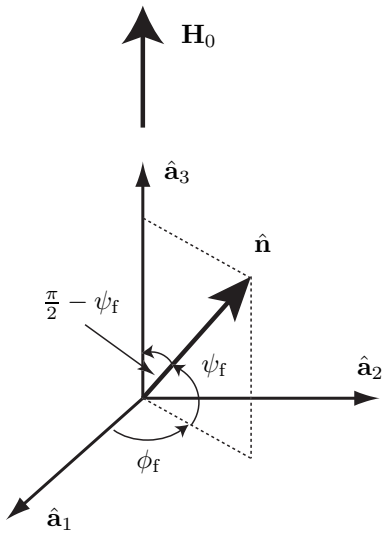


**Figure 3. A desired inertial direction $\hat{\mathbf{n}}$ in the inertial frame $\mathcal{H}$.**

Next, we provide an algorithm to find the values of the angles $\phi_{\mathrm{f}}$ and $\psi_{\mathrm{f}}$ (or $\gamma_{\mathrm{f}}$) in order to make the line-of-sight (herein, the $\hat{\mathbf{b}}_1$-axis) aim at an arbitrarily given direction $\hat{\mathbf{n}}$. To this end, suppose that $\hat{\mathbf{n}}$ can be written in the inertial frame $\mathcal{H}$ as $\hat{\mathbf{n}} = n_1\,\hat{\mathbf{a}}_1 + n_2\,\hat{\mathbf{a}}_2 + n_3\,\hat{\mathbf{a}}_3$. Then in order to make the body axis $\hat{\mathbf{b}}_1$ point at the inertial vector $\hat{\mathbf{n}}$, we require that

$$\begin{bmatrix} n_1 \\ n_2 \\ n_3 \end{bmatrix} = R_{\mathcal{B}}^{\mathcal{H}}\hat{\mathbf{b}}_1 = \begin{bmatrix} \cos\phi_{\mathrm{f}}\,\cos\psi_{\mathrm{f}} \\ \sin\phi_{\mathrm{f}}\,\cos\psi_{\mathrm{f}} \\ \sin\psi_{\mathrm{f}} \end{bmatrix}, \tag{12}$$

since $\cos\theta_\mathrm{f} = 0$ and $\sin\theta_\mathrm{f} = 1$. In fact, the right hand side of (12) is the expression of the vector $\hat{\mathbf{n}}$ in the spherical coordinate system, shown in Fig. 3. One can therefore specify the desired final value of the parameters $\phi_\mathrm{f}$ and $\psi_\mathrm{f}$ for any given inertial vector $\hat{\mathbf{n}}$.

Since $\hat{\mathbf{n}}$ is perpendicular to $\hat{\mathbf{a}}_2$ it follows that $n_2 = \sin\phi_\mathrm{f}\cos\psi_\mathrm{f} = 0$. There can be two possibilities for the final required attitude parameters. The first possibility is that $\cos\psi_\mathrm{f} = 0$, whereas $\phi_\mathrm{f}$ has any value. This solution implies that $n_1 = 0$ as well as $n_2 = 0$, and thus $n_3 = \pm 1$. This solution is valid only for the special case when the given inertial vector $\hat{\mathbf{n}}$ is parallel to $\mathbf{H}_0$. In general, one has that

$$\phi_\mathrm{f} = 0, \quad \psi_\mathrm{f} = \arctan\frac{n_1}{n_3}, \tag{13}$$

and hence this equation yields the final required values of the Euler angles for the majority of cases.

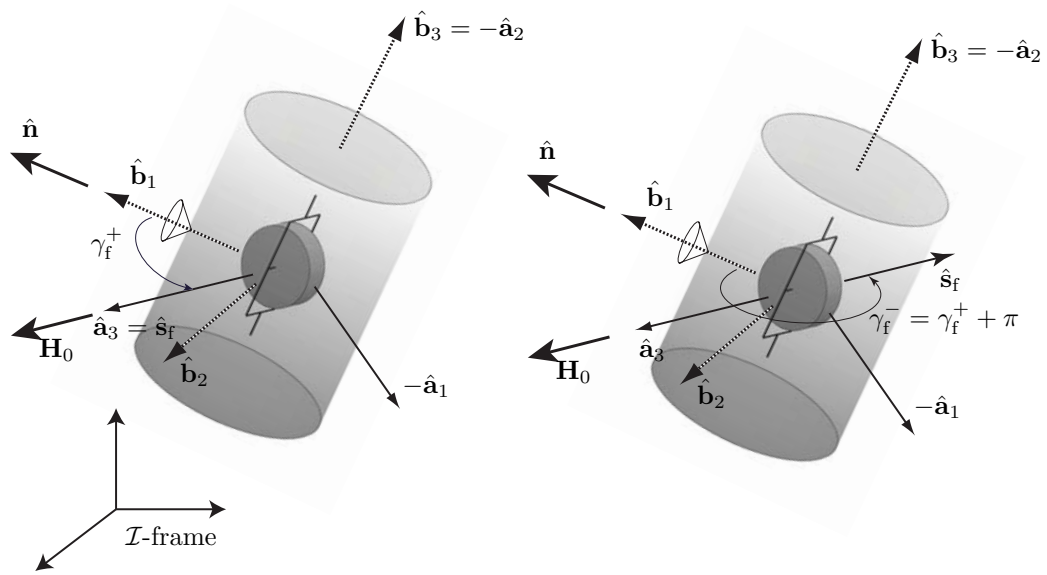


(a) $\Omega_\mathrm{f} = \Omega_\mathrm{f}^+ > 0$. (b) $\Omega_\mathrm{f} = \Omega_\mathrm{f}^- < 0$.

**Figure 4. Desired attitudes with $\boldsymbol{\omega} = 0$ for given $\mathbf{H}_0$ and $\hat{\mathbf{n}}$.**

Next, we show that a camera/anntena must be installed on the spacecraft so that its line-of-sight axis is normal to the gimbal axis in order to aim at an arbitrary inertial direction when $\boldsymbol{\omega} = 0$. To this end, let us define a body-fixed unit vector $\hat{\mathbf{b}} = b_1\hat{\mathbf{b}}_1 + b_2\hat{\mathbf{b}}_2 + b_3\hat{\mathbf{b}}_3$. When the spacecraft is at rest (and thus $\theta_\mathrm{f} = \pi/2$), the vector $\hat{\mathbf{b}}$ can be written in the $\mathcal{H}$-frame as $\hat{\mathbf{b}} = a_1\hat{\mathbf{a}}_1 + a_2\hat{\mathbf{a}}_2 + a_3\hat{\mathbf{a}}_3$, where

$$\begin{bmatrix} a_1 \\ a_2 \\ a_3 \end{bmatrix} = R_\mathcal{B}^\mathcal{H}\hat{\mathbf{b}} = \begin{bmatrix} \mathrm{c}\phi_\mathrm{f}\,\mathrm{c}\psi_\mathrm{f} & -\mathrm{c}\phi_\mathrm{f}\,\mathrm{s}\psi_\mathrm{f} & \mathrm{s}\phi_\mathrm{f} \\ \mathrm{s}\phi_\mathrm{f}\,\mathrm{c}\psi_\mathrm{f} & -\mathrm{s}\phi_\mathrm{f}\,\mathrm{s}\psi_\mathrm{f} & -\mathrm{c}\phi_\mathrm{f} \\ \mathrm{s}\psi_\mathrm{f} & \mathrm{c}\psi_\mathrm{f} & 0 \end{bmatrix} \begin{bmatrix} b_1 \\ b_2 \\ b_3 \end{bmatrix}. \tag{14}$$

In order to make $\hat{\mathbf{b}}$ point at the inertial direction $\hat{\mathbf{n}}$, the final Euler angles $\phi_\mathrm{f}$ and $\psi_\mathrm{f}$ must be such that $\hat{\mathbf{b}}\cdot\hat{\mathbf{n}} = a_1\,n_1 + a_2\,n_2 + a_3\,n_3 = 1$. In particular, let us consider the case when the line-of-sight axis (the $\hat{\mathbf{b}}$-axis) is commanded so that it aims at the direction of the total angular momentum, that is $\hat{\mathbf{n}} = \hat{\mathbf{a}}_3 = \mathbf{H}_0/H_0$. Then, $\hat{\mathbf{b}}\cdot\hat{\mathbf{n}} = \hat{\mathbf{b}}\cdot\hat{\mathbf{a}}_3 = a_3 = b_1\mathrm{s}\psi_\mathrm{f} + b_2\mathrm{c}\psi_\mathrm{f} = \sqrt{b_1^2 + b_2^2}\sin(\psi_\mathrm{f} + \alpha)$, where $\cos\alpha = b_1/\sqrt{b_1^2 + b_2^2}$, $\sin\alpha = b_2/\sqrt{b_1^2 + b_2^2}$. Since $\hat{\mathbf{b}}\cdot\hat{\mathbf{n}} = 1$ it follows that $b_1^2 + b_2^2 = 1$, and thus $b_3 = 0$, which implies that the body fixed vector $\hat{\mathbf{b}}$ must be perpendicular to the gimbal axis $\hat{\mathbf{b}}_3 = \hat{\mathbf{g}}$, thus completing the proof.

Figure 4 shows two final rest configurations for which $\hat{\mathbf{b}}_1$ points at the given inertial direction $\hat{\mathbf{n}}$. There are two possible cases, as expected from Eq. (11). One is with a positive final wheel speed, that is, $\Omega_\mathrm{f} = \Omega_\mathrm{f}^+ \triangleq H_0/I_\mathrm{ws} > 0$. In this case, the final gimbal axis $\hat{\mathbf{s}}_\mathrm{f}$ is aligned along $\mathbf{H}_0$ in the same direction, as shown in Fig. 4(a). The other case is with a negative final wheel speed, that is, $\Omega_\mathrm{f} = \Omega_\mathrm{f}^- \triangleq -H_0/I_\mathrm{ws} < 0$. The final gimbal spin axis $\hat{\mathbf{s}}_\mathrm{f}$ is aligned along $\mathbf{H}_0$ but has the opposite direction, as shown in Fig. 4(b).

In both cases, the final $\hat{\mathbf{b}}_1$-axis points at the direction of $\hat{\mathbf{n}}$, as desired. Notice that the gimbal axis $\hat{\mathbf{g}} = \hat{\mathbf{b}}_3$ is perpendicular to the total angular momentum vector $\mathbf{H}_0 = H_0\hat{\mathbf{a}}_3$ because $\theta_\mathrm{f} = \pi/2$. In fact, $\gamma_\mathrm{f}$ can be

computed by Eqs. (11) and (13) as

$$\gamma_{\rm f}^{+} = \arccos\left(\frac{\mathbf{H}_0 \cdot \hat{\mathbf{n}}}{H_0}\right), \qquad (\Omega_{\rm f} > 0), \tag{15a}$$

$$\gamma_{\rm f}^{-} = \gamma_{\rm f}^{+} - \pi, \qquad (\Omega_{\rm f} < 0). \tag{15b}$$

For each value of the sign of $\Omega_{\rm f}$ the pair $(\phi_{\rm f}, \gamma_{\rm f})$ determines the final spacecraft orientation at rest. Furthermore, if we design a controller that achieves

$$\boldsymbol{\omega} \to 0, \tag{16a}$$

$$\gamma_e \triangleq \gamma - \gamma_{\rm f} \to 0, \tag{16b}$$

$$\phi_e \triangleq \phi - \phi_{\rm f} \to 0, \tag{16c}$$

then the spacecraft will be brought to rest and the $\hat{\mathbf{b}}_1$-axis will point at the desired inertial direction $\hat{\mathbf{n}}$. Also, notice that in case $\hat{\mathbf{n}}$ is parallel to $\mathbf{H}_0$ the controller does not need to meet the last requirement in (16) since (16c) is redundant and can be ignored.

## IV. Linearized System Analysis and Controller Design

The kinematic differential equation for the "3-1-3" rotational sequence is given by

$$\begin{bmatrix} \dot{\phi} \\ \dot{\theta} \\ \dot{\psi} \end{bmatrix} = \frac{1}{\sin\theta} \begin{bmatrix} \mathrm{s}\psi & \mathrm{c}\psi & 0 \\ \mathrm{c}\psi\,\mathrm{s}\theta & -\mathrm{s}\psi\,\mathrm{s}\theta & 0 \\ -\mathrm{s}\psi\,\mathrm{c}\theta & -\mathrm{c}\psi\,\mathrm{c}\theta & \mathrm{s}\theta \end{bmatrix} \begin{bmatrix} \omega_1 \\ \omega_2 \\ \omega_3 \end{bmatrix}, \tag{17}$$

and the differential equation of $\gamma_e$ is

$$\dot{\gamma}_e = \dot{\gamma} = u_1. \tag{18}$$

In this section, we linearize the nonlinear equations of motion, given by (3), (17) and (18). We then use these equations to investigate the controllability properties of the system $(\boldsymbol{\omega}, \gamma_e, \phi_e)$. We also present an LQR control law that satisfies the control objectives (16) and thus stabilizes the angular velocity of spacecraft with a body-fixed axis aiming at a given inertial direction.

### A. Controllability Analysis

The desired equilibrium points of Eqs. (3),(17) and (18) are given by $\boldsymbol{\omega} = 0$, $\gamma_e = 0$, $\phi_e = 0$, $\Omega = \Omega_{\rm f}$ and $\mathbf{u} = [u_1,\ u_2]^T = 0$. Moreover, we know that $\sin\theta \approx 1$, $\sin\psi \approx \operatorname{sgn}\Omega_{\rm f}\cos\gamma$ and $\cos\psi \approx \operatorname{sgn}\Omega_{\rm f}\sin\gamma$ near the equilibrium. Thus one can linearize the differential equation of $\phi_e$ as follows.

$$\dot{\phi}_e = \dot{\phi} \approx (\omega_1\cos\gamma_{\rm f} + \omega_2\sin\gamma_{\rm f})\operatorname{sgn}\Omega_{\rm f} = \boldsymbol{\omega}\cdot\hat{\mathbf{s}}_{\rm f}\ \operatorname{sgn}\Omega_{\rm f}. \tag{19}$$

Therefore, we have two linearized systems depending on the sign of $\Omega_{\rm f}$, and the equations of motion are given by[35]

$$\begin{bmatrix} \dot{\boldsymbol{\omega}} \\ \dot{\gamma}_e \\ \dot{\phi}_e \end{bmatrix} = \begin{bmatrix} A_1 & 0 & 0 \\ 0 & 0 & 0 \\ A_2 & 0 & 0 \end{bmatrix} \begin{bmatrix} \Delta\boldsymbol{\omega} \\ \gamma_e \\ \phi_e \end{bmatrix} + \begin{bmatrix} B_1 & B_2 \\ 1 & 0 \\ 0 & 0 \end{bmatrix} \begin{bmatrix} u_1 \\ \operatorname{sgn}\Omega_{\rm f}\,u_2 \end{bmatrix} \tag{20}$$

where,

$$A_1 \triangleq J^{-1} I_{\rm ws}\Omega_{\rm f}\,\hat{\mathbf{s}}_{\rm f}^{\times} \tag{21a}$$

$$A_2 \triangleq \hat{\mathbf{s}}_{\rm f}^{T}\ \operatorname{sgn}\Omega_{\rm f} \tag{21b}$$

$$B_1 \triangleq -J^{-1} I_{\rm ws}\Omega_{\rm f}\,\hat{\mathbf{t}}_{\rm f} \tag{21c}$$

$$B_2 \triangleq -J^{-1} I_{\rm ws}\,\hat{\mathbf{s}}_{\rm f} \tag{21d}$$

where all vectors are expressed in the $\mathcal{B}$-frame.

**Proposition 1.** *The linearized system described by Eqs. (20) and (21) is controllable for any* $\gamma_{\mathrm{f}} \in [0, 2\pi)$ *and* $\Omega_{\mathrm{f}} \in \mathbb{R}\backslash\{0\}$.

*Proof.* The controllability of Eqs. (20) and (21) can be shown using the Popov-Belevitch-Hautus (PBH) test.[37] A necessary and sufficient condition for the controllability of (20) and (21) is that the matrix $\mathcal{C}(\lambda)$ defined as

$$\mathcal{C}(\lambda) \triangleq \begin{bmatrix} A_1 - \lambda I & 0 & 0 & B_1 & B_2 \\ 0 & -\lambda & 0 & 1 & 0 \\ A_2 & 0 & -\lambda & 0 & 0 \end{bmatrix} \tag{22}$$

has rank 5 for all $\lambda \in \mathbb{C}$. It can be easily proved using the approach of Ref. 35 that the linearized subsystem $(\boldsymbol{\omega}, \gamma_e)$ is controllable, that is, the pair of matrices $(\bar{A}, \bar{B})$, where

$$\bar{A} \triangleq \begin{bmatrix} A_1 & 0 \\ 0 & 0 \end{bmatrix}, \quad \bar{B} \triangleq \begin{bmatrix} B_1 & B_2 \\ 1 & 0 \end{bmatrix}, \tag{23}$$

is controllable.[38] Therefore, it follows easily that rank $\mathcal{C}(\lambda) = 5$ for all $\lambda \neq 0$. We only need to check the rank of the matrix

$$\mathcal{C}'(0) \triangleq \begin{bmatrix} A_1 & B_1 & B_2 \\ 0 & 1 & 0 \\ \hat{\mathbf{s}}_{\mathrm{f}}^T \operatorname{sgn}\Omega_{\mathrm{f}} & 0 & 0 \end{bmatrix}. \tag{24}$$

Notice that

$$\operatorname{rank} \mathcal{C}'(0) = \operatorname{rank} \begin{bmatrix} \hat{\mathbf{s}}_{\mathrm{f}}^{\times} & \hat{\mathbf{t}}_{\mathrm{f}} & \hat{\mathbf{s}}_{\mathrm{f}} \\ 0 & 1 & 0 \\ \hat{\mathbf{s}}_{\mathrm{f}}^T & 0 & 0 \end{bmatrix}. \tag{25}$$

To this end, assume that there exist a vector $\mathbf{v}_1 \in \mathbb{R}^3$, and scalars $v_2, v_3 \in \mathbb{R}$ such that

$$\begin{bmatrix} \mathbf{v}_1^T & v_2 & v_3 \end{bmatrix} \begin{bmatrix} \hat{\mathbf{s}}_{\mathrm{f}}^{\times} & \hat{\mathbf{t}}_{\mathrm{f}} & \hat{\mathbf{s}}_{\mathrm{f}} \\ 0 & 1 & 0 \\ \hat{\mathbf{s}}_{\mathrm{f}}^T & 0 & 0 \end{bmatrix} = 0. \tag{26}$$

Equivalently,

$$\mathbf{v}_1^T \hat{\mathbf{s}}_{\mathrm{f}}^{\times} + v_3 \hat{\mathbf{s}}_{\mathrm{f}}^T = 0, \tag{27}$$

$$\mathbf{v}_1^T \hat{\mathbf{t}}_{\mathrm{f}} + v_2 = 0, \tag{28}$$

$$\mathbf{v}_1^T \hat{\mathbf{s}}_{\mathrm{f}} = 0. \tag{29}$$

Equation (27) holds if and only if $\mathbf{v}_1 = 0$ and $v_3 = 0$. From (28) it follows that $v_2 = 0$. This implies that the left null space of the matrix in Eq. (26) contains only the zero vector and thus rank $\mathcal{C}'(0) = 5$ and the proof is completed. □

Notice that Proposition 1 does not ensure the controllability of the linearized system if $\Omega_{\mathrm{f}} = 0$. However, if the initial angular momentum $\mathbf{H}_0$ is not zero, then $\Omega_{\mathrm{f}} \neq 0$ by conservation of the angular momentum.

### B. Linear Control Design

Next, we design a linear control law via LQR theory for the linearized system (20). Let the matrices $A$ and $B$ denote the system matrices in Eq. (20). Then we can determine a control gain matrix $K \in \mathbb{R}^{2\times 5}$ such that the static full-state feedback law

$$\mathbf{u} = [u_1, \operatorname{sgn}\Omega_{\mathrm{f}}\, u_2]^T = -K[\boldsymbol{\omega}^T, \gamma_e, \phi_e]^T \tag{30}$$

minimizes the performance index

$$\mathcal{J} \triangleq \int_0^{\infty} \left(\mathbf{x}^T Q\, \mathbf{x} + \mathbf{u}^T R\, \mathbf{u}\right) \mathrm{d}t \tag{31}$$

where $\mathbf{x} = [\boldsymbol{\omega}^T, \gamma_e, \phi_e]^T$, $Q \in \mathbb{R}^{5\times5}$ is positive semi-definite, and $R \in \mathbb{R}^{2\times2}$ is positive definite. The gain matrix $K$ is computed by $K = R^{-1}B^TP$, where $P$ is the solution of the Algebraic Riccati Equation (ARE)

$$A^TP + PA - PBR^{-1}B^TP + Q = 0. \tag{32}$$

No further details are provided since LQR theory is well known in the literature.[39]

## V. Nonlinear System Analysis and Controller Design

The LQR controller of the previous section ensures asymptotic stability only locally about the equilibrium $\boldsymbol{\omega} = 0$ (and thus also $\Omega = \Omega_\mathrm{f}$), $\gamma_e = 0$ and $\phi_e = 0$. In realistic cases, however, one cannot expect that the initial states will be near the equilibrium point. In order to achieve the desired stabilization objective for all initial conditions at large (not necessarily close to the origin), it is necessary to design a controller based on the complete nonlinear equations of motion.

In the sequel we suggest a control methodology which is comprised of a sequence of three stages. At the first stage, only the angular velocity $\boldsymbol{\omega}$ is controlled to decrease toward zero. When a certain condition is met, the controller switches to the second stage in which both $\boldsymbol{\omega}$ and the gimbal angle $\gamma$ are controlled to the desired values, according to the sign of the wheel speed. Once $\boldsymbol{\omega}$ and $\gamma$ are sufficiently close to the values at the desired equilibrium, then the controller switches to the third stage where the LQR controller designed in Section IV regulates the Euler angle $\phi$ to $\phi_\mathrm{f}$, along with $\boldsymbol{\omega}$ and $\gamma$.

Several assumptions are made in order to simplify the analysis.

- **Assumption 1.** The spacecraft is inertially axisymmetric about the gimbal axis $\hat{\mathbf{g}} = \hat{\mathbf{b}}_3$.
- **Assumption 2.** The spacecraft is not inertially symmetric.

Under Assumption 1, the inertia matrix written in the gimbal frame $\mathcal{G}$ takes the form

$$J = \begin{bmatrix} J_\mathrm{t} & 0 & 0 \\ 0 & J_\mathrm{t} & 0 \\ 0 & 0 & J_\mathrm{a} \end{bmatrix}. \tag{33}$$

Assumption 2 implies that $J_\mathrm{t} \neq J_\mathrm{a}$.

### A. Angular Velocity Stabilization

Consider the positive definite, continuously differentiable Lyapunov function candidate

$$V_1(\boldsymbol{\omega}) = \tfrac{1}{2}\boldsymbol{\omega}^T J \boldsymbol{\omega}. \tag{34}$$

Its time derivative along the trajectories of the system (3) yields

$$\begin{aligned} \dot{V}_1 &= \boldsymbol{\omega}^T J \dot{\boldsymbol{\omega}} \\ &= \boldsymbol{\omega}^T \left( -\boldsymbol{\omega}^\times (J\boldsymbol{\omega} + I_\mathrm{cg}\dot{\gamma}\hat{\mathbf{g}} + I_\mathrm{ws}\Omega\hat{\mathbf{s}}) - I_\mathrm{ws}\Omega\hat{\mathbf{t}}u_1 - I_\mathrm{ws}\hat{\mathbf{s}}u_2 \right) \\ &= -\omega_\mathrm{t} I_\mathrm{ws}\Omega u_1 - I_\mathrm{ws}\omega_\mathrm{s} u_2 \end{aligned} \tag{35}$$

where $\omega_\mathrm{s} = \boldsymbol{\omega}^T\hat{\mathbf{s}}$ and $\omega_\mathrm{t} = \boldsymbol{\omega}^T\hat{\mathbf{t}}$ are the projections of the body angular velocity $\boldsymbol{\omega}$ along the spin and transverse axes of the gimbal frame, respectively, that is, $\boldsymbol{\omega} = \omega_\mathrm{s}\hat{\mathbf{s}} + \omega_\mathrm{t}\hat{\mathbf{t}} + \omega_\mathrm{g}\hat{\mathbf{g}}$, where $\omega_\mathrm{g} = \boldsymbol{\omega}^T\hat{\mathbf{g}}$. Taking a control law as

$$u_1 = \dot{\gamma} = k_1\omega_\mathrm{t} I_\mathrm{ws}\Omega, \quad k_1 > 0, \tag{36a}$$

$$u_2 = \dot{\Omega} = k_2 I_\mathrm{ws}\omega_\mathrm{s}, \quad k_2 > 0, \tag{36b}$$

yields

$$\dot{V}_1 = -k_1(\omega_\mathrm{t} I_\mathrm{ws}\Omega)^2 - k_2(I_\mathrm{ws}\omega_\mathrm{s})^2 \leq 0. \tag{37}$$

In order to show that the control law (36) provides a stabilizing feedback, we need to show that there exists $c_0 > 0$ such that, for each $c_1 \in (0, c_0)$, no trajectory of the vector field with $\mathbf{u} = 0$ is contained inside the set

$$\mathcal{L}_c \triangleq \{\boldsymbol{\omega} : V_1(\boldsymbol{\omega}) = c_1 \text{ and } \omega_\mathrm{t} I_\mathrm{ws}\Omega = I_\mathrm{ws}\omega_\mathrm{s} = 0\}. \tag{38}$$

In other words, we need to show that no trajectories of the control-free system stay in nontrivial invariant sets of $\dot{V}_1 = 0$, which are characterized by the equations

$$\omega_{\mathrm{t}} I_{\mathrm{ws}} \Omega = 0, \tag{39a}$$

$$I_{\mathrm{ws}} \omega_{\mathrm{s}} = 0. \tag{39b}$$

Inside the invariant set $\mathcal{L}_c$, we have that $u_1 = \dot{\gamma} = 0$ and $u_2 = \dot{\Omega} = 0$, and thus $\gamma$ and $\Omega$ are constant. In addition, $\omega_{\mathrm{s}} = 0$ from (39b). Because $\gamma$ is constant, the gimbal frame $\mathcal{G}$ is fixed in the body frame. Rewriting the dynamic equations in the $\mathcal{G}$-frame, one obtains

$$J\dot{\boldsymbol{\omega}} = -\boldsymbol{\omega}^{\times}(J\boldsymbol{\omega} + I_{\mathrm{ws}}\Omega\hat{\mathbf{s}}) = -\boldsymbol{\omega}^{\times}\mathbf{h}, \tag{40}$$

where

$$\boldsymbol{\omega} = [0, \omega_{\mathrm{t}}, \omega_{\mathrm{g}}]^T, \quad \dot{\boldsymbol{\omega}} = [0, \dot{\omega}_{\mathrm{t}}, \dot{\omega}_{\mathrm{g}}]^T. \tag{41}$$

Using Eqs. (33) and (41), Eq. (40) can be written as

$$\begin{bmatrix} 0 \\ J_{\mathrm{t}}\dot{\omega}_{\mathrm{t}} \\ J_{\mathrm{a}}\dot{\omega}_{\mathrm{g}} \end{bmatrix} = -\begin{bmatrix} h_3\omega_{\mathrm{t}} - h_2\omega_{\mathrm{g}} \\ h_1\omega_{\mathrm{g}} \\ -h_1\omega_{\mathrm{t}} \end{bmatrix} = \begin{bmatrix} \omega_{\mathrm{t}}\omega_{\mathrm{g}}(J_{\mathrm{t}} - J_{\mathrm{a}}) \\ -I_{\mathrm{ws}}\Omega\omega_{\mathrm{g}} \\ I_{\mathrm{ws}}\Omega\omega_{\mathrm{t}} \end{bmatrix}, \tag{42}$$

where

$$\mathbf{h} = [h_1, h_2, h_3]^T = [I_{\mathrm{ws}}\Omega, J_{\mathrm{t}}\omega_{\mathrm{t}}, J_{\mathrm{a}}\omega_{\mathrm{g}}]^T \tag{43}$$

is the total angular momentum of the vehicle expressed in the gimbal frame. Comparing the fist element in Eq. (42), one obtains $\omega_{\mathrm{t}}\omega_{\mathrm{g}} = 0$ for the equilibria. Also, one has $\omega_{\mathrm{t}}\Omega = 0$ from Eq. (39a). Thus, there are two different types of the equilibria: i) $\omega_{\mathrm{t}} = 0$, $\omega_{\mathrm{g}} \in \mathbb{R}$, and ii) $\omega_{\mathrm{g}} = \Omega = 0$, $\omega_{\mathrm{t}} \in \mathbb{R}$.

i) $\omega_{\mathrm{t}} = 0$, $\omega_{\mathrm{g}} \in \mathbb{R}$: Comparing the second element in Eq. (42), one has $\Omega\omega_{\mathrm{g}} = 0$. If $\omega_{\mathrm{g}} = 0$, then $\boldsymbol{\omega} = 0$, which is the desired equilibrium. However, there can still be a nontrivial equilibrium given by $\Omega = 0$, $\boldsymbol{\omega} = [0, 0, \pm H_0/J_{\mathrm{a}}]^T$.

ii) $\omega_{\mathrm{g}} = \Omega = 0$, $\omega_{\mathrm{t}} \in \mathbb{R}$: There can be a nontrivial equilibrium at $\Omega = 0$, $\boldsymbol{\omega} = [0, \pm H_0/J_{\mathrm{t}}, 0]^T$.

Therefore, there exist nontrivial equilibria contained inside the invariant set $\mathcal{L}_c$, thus global stabilization is not guaranteed. Nonetheless, these nontrivial equilibria are unstable; see Appendix A for the proof. Therefore, "essentially global stability" or "regional stability" (global stability except a nowhere dense subset) follows. This type of stability is all that is needed from a practical point of view.

### B. Stabilization of $\boldsymbol{\omega}$, $\gamma_e$ and $\Omega_e$

The nonlinear controller designed in the previous section stabilizes $\boldsymbol{\omega}$, but it cannot achieve the overall control objective, as it controls only the angular velocity vector. Hence, the final orientation of the spacecraft is not controlled. In this section, we design a nonlinear controller which makes, in addition to $\boldsymbol{\omega} \to 0$, also $\gamma_e = \gamma - \gamma_{\mathrm{f}} \to 0$.

Notice that there are two possible desired values of the final gimbal angle $\gamma_{\mathrm{f}}$ in this case, depending on the sign of the final wheel speed $\Omega_{\mathrm{f}}$, as shown in Eq. (11) or Eq. (15). The magnitude of the final wheel speed is given by $|\Omega_{\mathrm{f}}| = H_0/I_{\mathrm{ws}}$ as $\boldsymbol{\omega} \to 0$ due to the momentum conservation law, but its sign can be either positive or negative, unless it is explicitly controlled. Thus, we also need to control the wheel speed $\Omega$ as well as $\boldsymbol{\omega}$ and $\gamma$.

First, let us consider a nonlinear controller which makes $\boldsymbol{\omega} \to 0$, $\gamma \to \gamma_{\mathrm{f}}^+$ and $\Omega \to \Omega_{\mathrm{f}}^+$. For this purpose, define a Lyapunov function candidate $V_2^+(\boldsymbol{\omega}, \gamma_e, \Omega_e)$ as

$$\begin{aligned} V_2^+(\boldsymbol{\omega}, \gamma_e, \Omega_e) &\triangleq \tfrac{1}{2}\boldsymbol{\omega}^T J\boldsymbol{\omega} + \tfrac{1}{2}k_\gamma {\gamma_e^+}^2 + \tfrac{1}{2}k_\Omega {\Omega_e^+}^2 \\ &= \tfrac{1}{2}\left(J_{\mathrm{t}}(\omega_{\mathrm{s}}^2 + \omega_{\mathrm{t}}^2) + J_{\mathrm{a}}\omega_{\mathrm{g}}^2\right) + \tfrac{1}{2}k_\gamma {\gamma_e^+}^2 + \tfrac{1}{2}k_\Omega {\Omega_e^+}^2, \quad k_\gamma, k_\Omega > 0, \end{aligned} \tag{44}$$

where $\gamma_e^+ \triangleq \gamma - \gamma_{\rm f}^+$ and $\Omega_e^+ \triangleq \Omega - \Omega_{\rm f}^+$. Its time derivative along the trajectories of the system (3) and (18) yields

$$\begin{aligned}\dot{V}_2^+ &= \boldsymbol{\omega}^T J\dot{\boldsymbol{\omega}} + k_\gamma \gamma_e^+ \dot{\gamma} + k_\Omega \Omega_e^+ \dot{\Omega} \\ &= -(\omega_{\rm t} I_{\rm ws}\Omega - k_\gamma \gamma_e^+)u_1 - (I_{\rm ws}\omega_{\rm s} - k_\Omega \Omega_e^+)u_2.\end{aligned} \tag{45}$$

Choosing a control law as

$$u_1 = \dot{\gamma} = k_3(\omega_{\rm t} I_{\rm ws}\Omega - k_\gamma \gamma_e^+), \quad k_3 > 0, \tag{46a}$$

$$u_2 = \dot{\Omega} = k_4(I_{\rm ws}\omega_{\rm s} - k_\Omega \Omega_e^+), \quad k_4 > 0, \tag{46b}$$

yields

$$\dot{V}_2^+ = -k_3(\omega_{\rm t} I_{\rm ws}\Omega - k_\gamma \gamma_e)^2 - k_4(I_{\rm ws}\omega_{\rm s} - k_\Omega \Omega_e)^2 \leq 0. \tag{47}$$

Now, let us check whether there exist nontrivial equilibria which make $\dot{V}_2^+ = 0$, as we did in Section A. These equilibria are characterized by the equations

$$\omega_{\rm t} I_{\rm ws}\Omega - k_\gamma \gamma_e = 0 \quad \text{and} \quad I_{\rm ws}\omega_{\rm s} - k_\Omega \Omega_e = 0. \tag{48}$$

There are three types of nontrivial equilibria, and are shown in Table 1. See Appendix B for the details.

**Table 1. Nontrivial Equilibria of the System under Controller Eq. (46).**

| Type | E1 | E2 | E3 |
|---|---|---|---|
| $\omega_{\rm s}$ | $-\frac{k_\Omega H_0}{I_{\rm ws}^2}$ | $-\frac{2H_0}{J_{\rm t}+I_{\rm ws}^2/k_\Omega}$ | $\frac{H_0}{J_{\rm a}-J_{\rm t}-I_{\rm ws}^2/k_\Omega}$ |
| $\omega_{\rm t}$ | $\pm\sqrt{\frac{H_0^2}{I_{\rm ws}^4}\left(\frac{I_{\rm ws}^4}{J_{\rm t}^2} - k_\Omega^2\right)}$ | 0 | 0 |
| $\omega_{\rm g}$ | 0 | 0 | $\pm\sqrt{H_0^2\left(\frac{1}{J_{\rm a}^2} - \frac{1}{(J_{\rm a}-J_{\rm t}-I_{\rm ws}^2/k_\Omega)^2}\right)}$ |
| $\gamma_e$ | 0 | 0 | 0 |
| $\Omega$ | 0 | $\frac{-2I_{\rm ws}H_0}{J_{\rm t}k_\Omega+I_{\rm ws}^2} + \frac{H_0}{I_{\rm ws}}$ | $-\frac{I_{\rm ws}H_0}{k_\Omega(J_{\rm t}-J_{\rm a})+I_{\rm ws}^2} + \frac{H_0}{I_{\rm ws}}$ |
| $V_2^+$ | $\frac{1}{2}H_0^2\left(\frac{1}{J_{\rm t}} + \frac{k_\Omega}{I_{\rm ws}^2}\right)$ | $\frac{2k_\Omega H_0^2}{I_{\rm ws}^2+k_\Omega J_{\rm t}}$ | $\frac{1}{2}\frac{H_0^2(I_{\rm ws}^2+k_\Omega J_{\rm t})}{J_{\rm a}(k_\Omega(J_{\rm t}-J_a)+I_{\rm ws}^2)}$ |

Similarly, we also consider a nonlinear controller for the negative final wheel speed $\Omega_{\rm f}^-$. Define another Lyapunov function candidate $V_2^-(\boldsymbol{\omega}, \gamma_e, \Omega_e)$ as

$$\begin{aligned}V_2^-(\boldsymbol{\omega}, \gamma_e, \Omega_e) &\triangleq \tfrac{1}{2}\boldsymbol{\omega}^T J\boldsymbol{\omega} + \tfrac{1}{2}k_\gamma {\gamma_e^-}^2 + \tfrac{1}{2}k_\Omega {\Omega_e^-}^2 \\ &= \tfrac{1}{2}\left(J_{\rm t}(\omega_{\rm s}^2 + \omega_{\rm t}^2) + J_{\rm a}\omega_{\rm g}^2\right) + \tfrac{1}{2}k_\gamma {\gamma_e^-}^2 + \tfrac{1}{2}k_\Omega {\Omega_e^-}^2,\end{aligned} \tag{49}$$

where $\gamma_e^- \triangleq \gamma - \gamma_{\rm f}^-$ and $\Omega_e^- \triangleq \Omega - \Omega_{\rm f}^-$. This Lyapunov function candidate suggests the control law

$$u_1 = \dot{\gamma} = k_3(\omega_{\rm t} I_{\rm ws}\Omega - k_\gamma \gamma_e^-), \quad k_3 > 0, \tag{50a}$$

$$u_2 = \dot{\Omega} = k_4(I_{\rm ws}\omega_{\rm s} - k_\Omega \Omega_e^-), \quad k_4 > 0. \tag{50b}$$

One can show that the nontrivial equilibria of this control law are identical with those of the control law (46) shown in Table 1, except that $\omega_{\rm s}$ and $\Omega$ have opposite sign.

Since it is rather complicated to check the stability of these nontrivial equilibria using Lyapunov's first method as did in Section A, here we follow a different approach. We eliminate the possibility of encountering these nontrivial equilibria altogether, by properly choosing the values of the controller gains, and by utilizing the controller designed in Section A, which stabilizes the angular velocity $\boldsymbol{\omega}$. To this end, let $V_{2\rm eq}$ be the minimum of the values of Lyapunov candidates $V_2^+$ and $V_2^-$ at the nontrivial equilibria, that is, let

$$V_{2\rm eq} \triangleq \min\{\tfrac{1}{2}H_0^2\left(\tfrac{1}{J_{\rm t}} + \tfrac{k_\Omega}{I_{\rm ws}^2}\right),\ \tfrac{2k_\Omega H_0^2}{I_{\rm ws}^2+k_\Omega J_{\rm t}},\ \tfrac{1}{2}\tfrac{H_0^2(I_{\rm ws}^2+k_\Omega J_{\rm t})}{J_{\rm a}(k_\Omega(J_{\rm t}-J_a)+I_{\rm ws}^2)}\}. \tag{51}$$

For any nonzero initial angular momentum $\mathbf{H}_0$ and any spacecraft inertia matrix $J$, we can choose the control gains $k_\gamma$ and $k_\Omega$ so that

$$V_{2\text{eq}} > \tfrac{1}{2} k_\gamma \pi^2. \tag{52}$$

If we take the value of the gimbal angle $\gamma$ using the "congruence"-function modulo $2\pi$, that is,

$$\begin{aligned} \gamma^+ = &\quad \text{mod}(\gamma + \pi - \gamma_\text{f}^+, 2\pi) - \pi + \gamma_\text{f}^+, \\ \gamma^- = &\quad \text{mod}(\gamma + \pi - \gamma_\text{f}^-, 2\pi) - \pi + \gamma_\text{f}^-, \end{aligned} \tag{53}$$

and redefine

$$\gamma_e^+ \triangleq \gamma^+ - \gamma_\text{f}^+, \quad \gamma_e^- \triangleq \gamma^- - \gamma_\text{f}^-, \tag{54}$$

then the gimbal angle errors are confined as $-\pi \le \gamma_e^+ < \pi$ and $-\pi \le \gamma_e^- < \pi$.

Now, suppose that the control law (36) is applied to make $\boldsymbol{\omega} \to 0$. From momentum conservation, the wheel speed $\Omega$ converges to either $\Omega_\text{f}^+$ or $\Omega_\text{f}^-$, as $\boldsymbol{\omega} \to 0$. If we let $\epsilon \triangleq V_{2\text{eq}} - \frac{1}{2} k_\gamma \pi^2 > 0$ from Eq. (52), then there exist a time $t_\text{s} > 0$ such that

$$\tfrac{1}{2}(\boldsymbol{\omega}^T J \boldsymbol{\omega} + k_\Omega {\Omega_e^+}^2)\Big|_{t=t_\text{s}} < \epsilon, \quad \text{or} \quad \tfrac{1}{2}(\boldsymbol{\omega}^T J \boldsymbol{\omega} + k_\Omega {\Omega_e^-}^2)\Big|_{t=t_\text{s}} < \epsilon. \tag{55}$$

At this time $t_\text{s}$, therefore, one of the following equations must hold

$$V_2^+(t=t_\text{s}) < \epsilon + \tfrac{1}{2} k_\gamma {\gamma_e^+}^2 < \epsilon + \tfrac{1}{2} k_\gamma \pi^2 = V_{2\text{eq}}, \tag{56a}$$

$$V_2^-(t=t_\text{s}) < \epsilon + \tfrac{1}{2} k_\gamma {\gamma_e^-}^2 < \epsilon + \tfrac{1}{2} k_\gamma \pi^2 = V_{2\text{eq}}. \tag{56b}$$

Hence, if we switch the controller at $t = t_\text{s}$ from Eq. (36) to Eqs. (46) or (50), depending on the sign of the wheel speed $\Omega$, then we ensure that $\gamma \to \gamma_\text{f}^+$ and $\Omega \to \Omega_\text{f}^+$, or $\gamma \to \gamma_\text{f}^-$ and $\Omega \to \Omega_\text{f}^-$ as $\boldsymbol{\omega} \to 0$, respectively, without encountering any of the nontrivial equilibria. This follows from the fact that the control laws (46) and (50) imply $\dot{V}_2^+ \le 0$ and $\dot{V}_2^- \le 0$ respectively.

**Remark 1** Inequality (52) imposes a restriction on the controller gain $k_\gamma$ which depends on the initial conditions for $H_0$, equivalently $\|\omega(0)\|$. For every bounded set of initial conditions the controller gain can be chosen such that this inequality is satisfied. This type of stability is better known in the literature as semi-global stability.

### C. Nonlinear control design for stabilization of $\boldsymbol{\omega}$, $\gamma_e$ and $\phi_e$

The final goal of the control design is to stabilize $\phi_e$, as well as $\boldsymbol{\omega}$ and $\gamma_e$. We already have designed three separate controllers, which we will utilize to fulfill this objective. One is a linear controller, designed in Section IV, which locally stabilizes $\boldsymbol{\omega}$, $\gamma_e$ and $\phi_e$. The second one is a nonlinear controller, designed in Section A, which regionally stabilizes $\boldsymbol{\omega}$. The third one designed in Section B makes $\boldsymbol{\omega} \to 0$, as well as $\gamma \to \gamma_\text{f}$ and $\Omega \to \Omega_\text{f}$. Each one of the first and the third controllers has two different versions according to the sign of $\Omega_\text{f}$. Utilizing these three control laws, we can construct a control logic consisting of three control phases that regionally achieves the final control objectives, given in Eq. (16). At the first stage, we use the nonlinear controller (36) to make $\boldsymbol{\omega} \to 0$. While this controller is being applied, the values of $V_2^+$ and $V_2^-$ are monitored, and if one of them becomes less than $V_{2\text{eq}}$, then the control switches to the second stage, where the controller (46) or (50) results in $\boldsymbol{\omega} \to 0$ and $\gamma \to \gamma_\text{f}$ where $\gamma_\text{f} = \gamma_\text{f}^+$ or $\gamma_\text{f}^-$, and $\Omega \to \Omega_\text{f}$ where $\Omega_\text{f} = \Omega_\text{f}^+$ or $\Omega_\text{f}^-$, according to the sign of $\Omega_\text{f}$. At the third stage, we use the linear controller in Section IV to also stabilize $\phi_e$ as well as $\boldsymbol{\omega}$,$\gamma_e$.

In order to use the linear controller in the third stage, we need all the states to be kept close to their desired equilibrium values, except $\phi_e$ which is ignorable, that is, it has no effect on the kinetic equations. It follows that $\boldsymbol{\omega} \approx 0, \gamma_e \approx 0, \Omega \approx \Omega_\text{f}$ at the beginning of and during the third stage. Owing to the nonlinear controller used at the second stage, $\boldsymbol{\omega}$ and $\gamma_e$ are stabilized at the beginning of the third stage. The wheel speed $\Omega$ also becomes $\Omega = \Omega_\text{f}$ to conserve the total angular momentum. In addition, if we determine the weighting matrix $Q$ and $R$ in the performance index (31) so that the weights on $\boldsymbol{\omega}$ and $\gamma_e$ are large, then the LQR controller which minimizes the performance index in (31) will keep $\boldsymbol{\omega}$ and $\gamma_e$ small during the third stage. The wheel speed variation also must be kept small, i.e., $\Omega \approx \Omega_\text{f}$, but this is not guaranteed by the LQR controller. From the momentum conservation law, however, if we can keep $\boldsymbol{\omega}$ sufficiently small during the third stage (by giving a large weight on $\boldsymbol{\omega}$ in the LQR controller), then $\Omega$ will also stay close to $\Omega_\text{f}$. Figure 5 summarizes the whole control procedure to achieve the control objective.

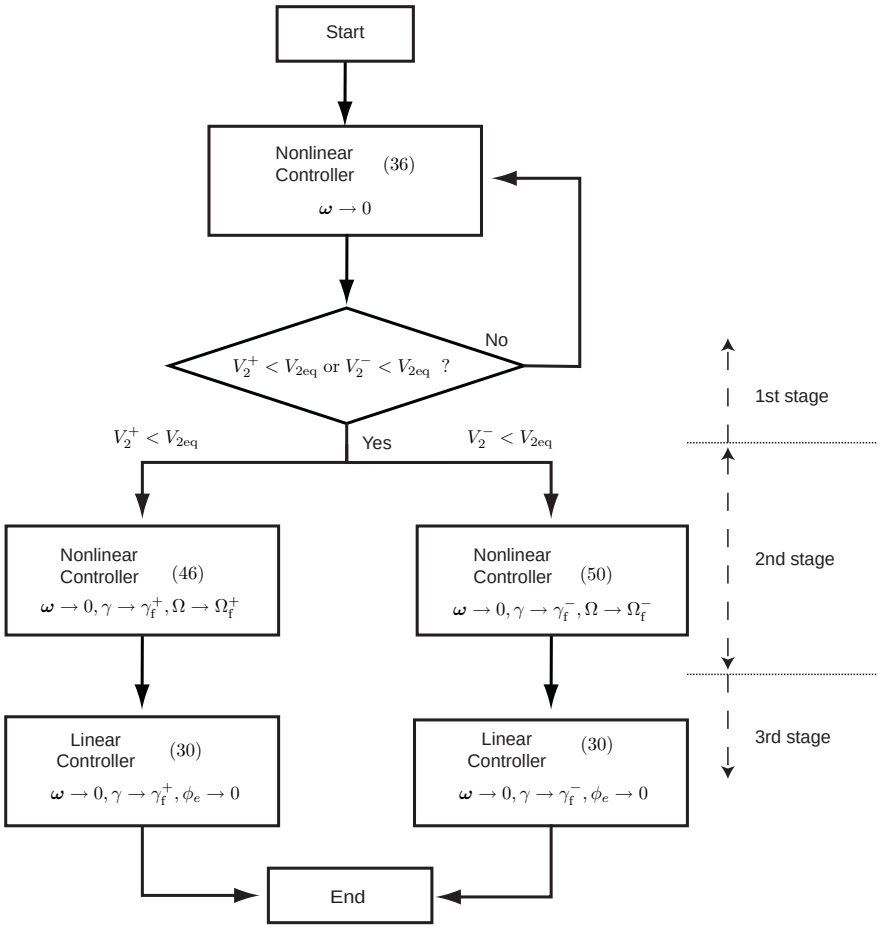


**Figure 5. Flow Chart of Entire Control Procedure.**

## VI. Numerical Examples

In this section, we give an illustrative example of the proposed control design method for the spacecraft angular velocity stabilization with the body-fixed line-of-sight control problem. In the previous sections, the simplified equations of motion with the assumptions $\dot{J} = 0$ and $I_{\text{cg}}\ddot{\gamma}\hat{\mathbf{g}} = 0$ were used for control design. In this section the complete nonlinear equations of motion given by Eq. (1) and the acceleration steering law of Refs. 33 and 35 are used to predict and validate the performance of the proposed controllers under realistic conditions. Table 2 summarizes the values of the moments of inertia of the spacecraft and the VSCMG used in all numerical simulations.

The control design parameters, the initial conditions and the desired line-of-sight $\hat{\mathbf{n}}$ used in the simulations are given in Table 3. To describe the attitude of the spacecraft with respect to the inertial frame $\mathcal{I}$, we use the Euler's parameters. The initial values of the quaternion vector in Table 3 implies that the initial body frame $\mathcal{B}$ is aligned with the inertial frame $\mathcal{I}$ at $t = 0$. The controller gains of the nonlinear controller and the weights of the LQR controller are chosen by trial and error in order to stabilize the system quickly and with suitable damping. In particular, the gains $k_\gamma$ and $k_\Omega$ are chosen so that the condition (52) holds.

For the given initial angular velocity $\boldsymbol{\omega}(0)$ and the line-of-sight direction vector $\hat{\mathbf{n}}$, the desired final gimbal angles are calculated from Eq. (15) as $\gamma_{\text{f}}^+ = 149.7^\circ$ and $\gamma_{\text{f}}^- = -30.3^\circ$. The final wheel speeds are given by $\Omega_{\text{f}}^+ = H_0/I_{\text{ws}} = 13606$ rpm and $\Omega_{\text{f}}^- = -H_0/I_{\text{ws}} = -13606$ rpm. In addition, the inertial frame $\mathcal{H}$, defined from (7) and (8), is given via

$$R_{\mathcal{I}}^{\mathcal{H}} = \begin{bmatrix} \hat{\mathbf{a}}_1^T \\ \hat{\mathbf{a}}_2^T \\ \hat{\mathbf{a}}_3^T \end{bmatrix} = \begin{bmatrix} 0.8889 & 0.4474 & 0.0983 \\ -0.1458 & 0.0729 & 0.9866 \\ 0.4342 & -0.8914 & 0.1300 \end{bmatrix}. \tag{57}$$

**Table 2. Spacecraft model parameters.**

| Symbol | Value | Units |
|---|---|---|
| ${}^{B}I$ | $\begin{bmatrix} 20 & 0 & 0 \\ 0 & 20 & 0 \\ 0 & 0 & 10 \end{bmatrix}$ | $\mathrm{kg\,m^2}$ |
| $I_{\mathrm{ws}}$ | 0.0042 | $\mathrm{kg\,m^2}$ |
| $I_{\mathrm{wt}}, I_{\mathrm{wg}}$ | 0.0024 | $\mathrm{kg\,m^2}$ |
| $I_{\mathrm{gs}}$ | 0.0093 | $\mathrm{kg\,m^2}$ |
| $I_{\mathrm{gt}}, I_{\mathrm{gg}}$ | 0.0054 | $\mathrm{kg\,m^2}$ |
| $\hat{\mathbf{s}}_0$ | $[1,0,0]^T$ | - |
| $\hat{\mathbf{t}}_0$ | $[0,1,0]^T$ | - |
| $\hat{\mathbf{g}}_0$ | $[0,0,1]^T$ | - |

**Table 3. Control design parameters and initial conditions.**

| Symbol | Value | Units |
|---|---|---|
| $\mathbf{q}(0)$ | $[0,0,0,1]^T$ | - |
| $\boldsymbol{\omega}(0)^*$ | $[-0.3,-0.2,0.1]^T$ | rad/sec |
| $\gamma(0)$ | 30 | deg |
| $\dot{\gamma}(0)$ | 0 | deg/sec |
| $\Omega(0)$ | $3\times10^3$ | rpm |
| $\hat{\mathbf{n}}^{**}$ | $\frac{1}{\sqrt{5}}[1,2,0]^T$ | - |
| $Q$ | $\mathrm{diag}[10^4,10^4,10^4,10^3,10^3]$ | - |
| $R$ | $\mathrm{diag}[10^3,1]$ | - |
| $k_1,\ k_3$ | 1 | - |
| $k_2,\ k_4$ | $5\times10^4$ | - |
| $k_\gamma$ | 0.05 | - |
| $k_\Omega$ | $1\times10^{-6}$ | - |
| $K_p$ | 1 | - |

* Written in the body frame $\mathcal{B}$

** Written in the inertial frame $\mathcal{I}$

Figures 6-11 show the results of the numerical simulations. As mentioned in Section C, the whole control procedure consists of three stages. During the first stage, the nonlinear controller (36) is applied so as to stabilize $\boldsymbol{\omega}$, while $\gamma$ and $\phi$ are allowed to take any values. For this example, $V_2^-$ becomes less than $V_{2\text{eq}} = 3.1487$ at $t_{\text{s1}} \approx 4.98$ sec, as shown in Fig. 7, so the control mode is switched to the second stage of the nonlinear controller (50). During the second stage, $\boldsymbol{\omega}$ is still under stabilization, and $\gamma \to \gamma_{\text{f}}^-$ and $\Omega \to \Omega_{\text{f}}^-$.

The switching from the second stage to the third stage occurs when the norms of $\boldsymbol{\omega}$ and $\gamma_e$ become smaller than some given tolerances $\epsilon_\omega, \epsilon_\gamma > 0$, respectively. We have used $\epsilon_\omega = 10^{-3}$ and $\epsilon_\gamma = 10^{-2}$ in the simulations, and the switching time for these tolerance was $t_{\text{s2}} \approx 110.66$ sec. At the third stage, the linear LQR controller is applied to achieve the overall control objective by making $\boldsymbol{\omega}$, $\gamma_e$ and $\phi_e$ all converge to zero.

Figure 6 shows the angular velocity trajectory of the spacecraft. As expected, the angular velocity is stabilized, then momentarily diverges after the switching from the second to the third stage (near $t_{\text{s2}} = 110.66$ sec), and converges to zero again. Notice that $\omega_3 = \omega_{\text{g}}$ is kept small even during the third stage. This means that the spacecraft does not rotate significantly about the gimbal axis, but it does rotate about the spin axis in order to make $\phi_e \to 0$. On the other hand, the other two angular velocity elements noticeably increase during the transition to the third stage. This increase can be mitigated by a suitable choice of the matrices $Q$ and $R$ in Eq. (31).

Figure 8 shows the attitude history of the body frame $\mathcal{B}$. Figure 8(a) is the time history of the quaternion parameters of $\mathcal{B}$ with respect to $\mathcal{I}$. Before the switching from the second to the third stage, the attitude parameters converge to certain constant values because $\boldsymbol{\omega} \to 0$ due to the nonlinear controller, and after switching, they converge to some other values as $\boldsymbol{\omega} \to 0$ again, due to the linear LQR controller. The final quaternion coincides with the desired final quaternion vector. Specifically, we may check that the final $\hat{\mathbf{b}}_1$-axis is

$$\hat{\mathbf{b}}_1 = [0.4472,\ 0.8944,\ 0]^T \approx \hat{\mathbf{n}}$$

which means that the line-of-sight fixed along the $\hat{\mathbf{b}}_1$-axis points at the given direction $\hat{\mathbf{n}}$, as desired.

Figures 8(b)-8(d) show the time history of the Euler angles of $\mathcal{B}$ with respect to $\mathcal{H}$, which are used for the parametrization of the spacecraft orientation at rest. As the angular velocity converges to zero, $\theta$ converges to $\theta_{\text{f}} = 90^\circ$ as expected. As shown in Fig. 8(b), $\phi$ is not controlled during the first and second stage, but after switching to the third stage, $\phi$ converges to zero as expected in Eq. (13) via the use of the LQR controller. The other Euler angle $\psi$ also converges to $\psi_{\text{f}} = -37.09^\circ$ given in Eq. (13). We can see that only $\phi$ varies in the third stage while $\theta$ and $\psi$ are nearly kept constant, and this implies again that the spacecraft rotates about the spin axis in the third stage.

Figure 9 shows the gimbal angle and the wheel speed trajectories of the VSCMG, respectively. It can be shown that both the gimbal angle changes and the wheel speed changes are exploited by the controller during the first and second stages to stabilize $\boldsymbol{\omega}$ and $\gamma_e$. However, in the third stage, only the wheel speed change is exploited to make $\phi \to 0$. The variation of the wheel speed in the third stage is not very large, so the use of the linearized analysis is justified. In fact, we can make the difference $\Omega - \Omega_{\text{f}}$ much smaller by weighting less $\phi$ or weighting more $\boldsymbol{\omega}$ and/or $\dot{\Omega}$ in the performance index (31), but then the convergence rate of $\phi$ will become slower in this case. It is also shown that the gimbal angle $\gamma$ converges to $\gamma_{\text{f}}^- = -52.91^\circ$, which satisfies Eq. (11). Figure 10 shows the trajectories of the control inputs, $\dot{\gamma}$ and $\dot{\Omega}$, as well the gimbal acceleration $\ddot{\gamma}$.

Finally, Fig. 11 shows a series of snapshots of the whole maneuver of the spacecraft. Note that the total angular momentum vector $\mathbf{H}$ is fixed in inertial space during the maneuver. The angular velocity $\boldsymbol{\omega}$ is gradually reduced to zero and it is hardly seen in these snapshots after $t = 40$ sec. At $t = 100$ sec., which is just before the switching from the second to the third stage, the gimbal angle $\gamma$ is $\gamma_{\text{f}}^- = -52.91^\circ$. See the relative positions of $\hat{\mathbf{b}}_1$ and $\hat{\mathbf{s}}$ about the $\hat{\mathbf{b}}_3$-axis. The spin axis $\hat{\mathbf{s}}$ is perfectly opposite in direction to $\mathbf{H}$, and the wheel speed is $\Omega = \Omega_{\text{f}}^- < 0$, which means that the wheel is actually spinning in the direction of $\mathbf{H}$ to conserve the angular momentum. At $t = 120$ sec., which is just after the second switching, we may see that the spacecraft rotates about the $\hat{\mathbf{s}}$-axis to align the $\hat{\mathbf{b}}_1$-axis with $\hat{\mathbf{n}}$, while controlled by the LQR controller. Near $t = 200$ sec., the spacecraft is at rest with the $\hat{\mathbf{b}}_1$-axis pointing at $\hat{\mathbf{n}}$, and the control objective is successfully achieved.

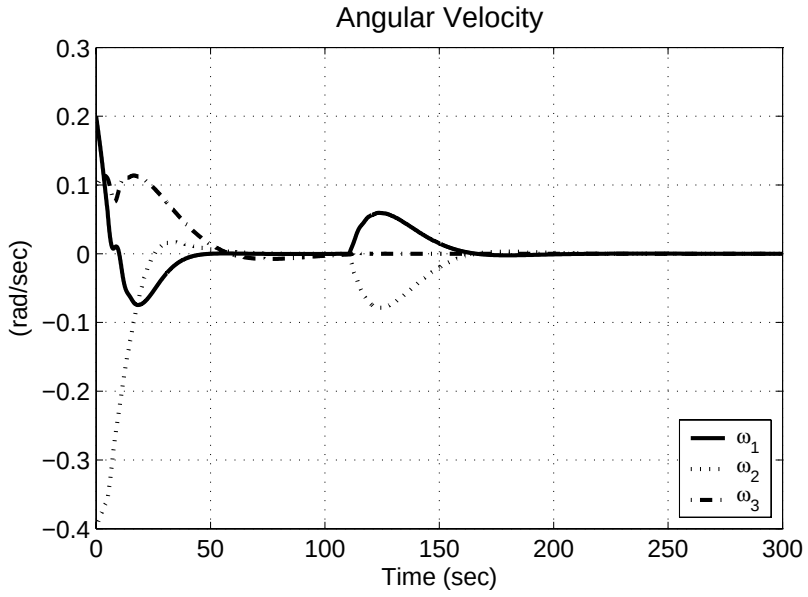


**Figure 6. Spacecraft angular velocity history $\boldsymbol{\omega}(t)$.**

## VII. Conclusions

The present paper deals with the attitude control problem of a rigid spacecraft using a single VSCMG. It is shown that the complete attitude equations are not controllable, but a certain type of partial attitude control without violating the angular momentum conservation principle is possible. As an example of partial attitude control, the control of a body-fixed line-of-sight is addressed. The approach is based on the complete characterization of all feasible final orientations of the spacecraft at rest by a single pair of two angles. Both linear (for small initial conditions) and nonlinear (for large initial conditions) strategies are presented. The proposed nonlinear control strategy consists of three consecutive stages and it successfully stabilizes the spacecraft angular velocity at large, while making the spacecraft line-of-sight aim at a given inertial direction. The results of this paper should be useful for spacecraft missions where only two-axis stabilization is of interest (e.g., the direction of a camera/antenna) or for mitigating actuator failures.

**Acknowledgement:** Support for this work was provided in part by AFOSR award F49620-00-1-0374.

## Appendix A : Instability of the Nontrivial Equilibria

In this Appendix, we show that the nontrivial equilibrium states of Eqs. (3) and (36) are unstable. For simplicity of the ensuing analysis, we assume that $\mathbf{h} \triangleq J\boldsymbol{\omega} + I_{\rm cg}\dot{\gamma}\hat{\mathbf{g}} + I_{\rm ws}\Omega\hat{\mathbf{s}} \approx J\boldsymbol{\omega} + I_{\rm ws}\Omega\hat{\mathbf{s}}$, which is justified by the fact that the gimbal angle rate $\dot{\gamma}$ does not contribute significantly to the total angular momentum. The closed-loop system with the proposed nonlinear controller (36) can be written as

$$J\dot{\boldsymbol{\omega}} = -\boldsymbol{\omega}^{\times}(J\boldsymbol{\omega} + I_{\rm ws}\Omega\hat{\mathbf{s}}) - k_1 I_{\rm ws}^2\Omega^2\omega_{\rm t}\hat{\mathbf{t}} - k_2 I_{\rm ws}^2\omega_{\rm s}\hat{\mathbf{s}} \tag{A.1}$$

$$\dot{\gamma} = k_1 I_{\rm ws}\Omega\omega_{\rm t} \tag{A.2}$$

$$\dot{\Omega} = k_2 I_{\rm ws}\omega_{\rm s} \tag{A.3}$$

Linearizing these equations about $\Omega = 0, \gamma_e = 0, \omega_{\rm t} = 0$ and $\omega_{\rm g} = \pm H_0/J_{\rm a}$, one obtains

$$J\Delta\dot{\boldsymbol{\omega}} = \left((J\boldsymbol{\omega})^{\times} - \boldsymbol{\omega}^{\times}J - k_2 I_{\rm ws}^2\hat{\mathbf{s}}\hat{\mathbf{s}}^T\right)\Delta\boldsymbol{\omega} - \boldsymbol{\omega}^{\times}I_{\rm ws}\hat{\mathbf{s}}\Delta\Omega \tag{A.4}$$

$$\Delta\dot{\gamma} = 0 \tag{A.5}$$

$$\Delta\dot{\Omega} = k_2 I_{\rm ws}\hat{\mathbf{s}}^T\Delta\boldsymbol{\omega} \tag{A.6}$$

It is obvious that the dynamics of $\Delta\gamma$ in Eq. (A.5) is neutrally stable, and can be decoupled from those of $\Delta\boldsymbol{\omega}$ and $\Delta\Omega$. Thus we only need to check the stability of Eqs. (A.4) and (A.6). It can be easily shown that

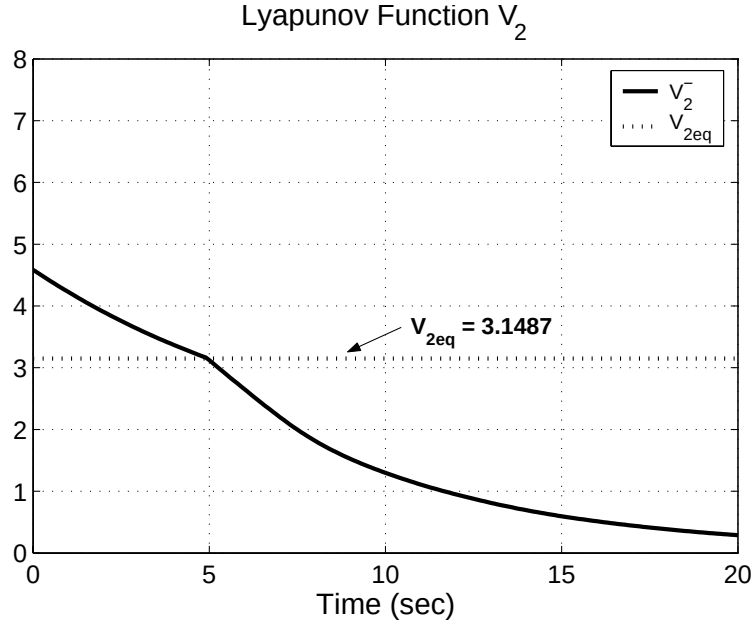


**Figure 7. Lyapunov function candidate history $V_2^-(t)$.**

the characteristic equation of this linear system is

$$\lambda(\lambda^3 + a_2\lambda^2 + a_1\lambda + a_0) = 0 \tag{A.7}$$

where

$$a_2 = (1/J_{\rm t})k_2 I_{\rm ws}^2, \quad a_1 = \frac{H_0^2(J_{\rm a} - J_{\rm t})^2}{J_{\rm t}^2 J_{\rm a}^2}, \quad a_0 = -\frac{I_{\rm ws}^2 k_2 H_0^2(J_{\rm a} - J_{\rm t})}{J_{\rm t}^2 J_{\rm a}^2}.$$

This equation has a single root at the origin, so the system is marginally stable at best. From Routh's stability criterion, a necessary and sufficient condition for stability for the characteristic equation (A.7) is

$$a_0 > 0, \quad a_1 > 0, \quad a_2 > 0$$

and

$$a_2 a_1 - a_0 = \frac{I_{\rm ws}^2 k_2 H_0^2(J_{\rm a} - J_{\rm t})}{J_{\rm a} J_{\rm t}^3} > 0$$

Note however that $a_0$ and $(a_2 a_1 - a_0)$ cannot have a same sign. Therefore, this equilibrium is unstable.

Similarly, consider the equilibrium $\Omega = 0, \gamma_e = 0, \omega_{\rm g} = 0$ and $\omega_{\rm t} = \pm H_0/J_{\rm t}$. The linearized equations about this equilibrium state are

$$J\Delta\dot{\boldsymbol{\omega}} = \left((J\boldsymbol{\omega})^\times - \boldsymbol{\omega}^\times J - k_2 I_{\rm ws}^2 \hat{\mathbf{s}}\hat{\mathbf{s}}^T\right)\Delta\boldsymbol{\omega} - k_2 I_{\rm ws}^2 \omega_{\rm t}\hat{\mathbf{s}}\Delta\gamma - \boldsymbol{\omega}^\times I_{\rm ws}\hat{\mathbf{s}}\Delta\Omega \tag{A.8}$$

$$\Delta\dot{\gamma} = k_1\omega_{\rm t} I_{\rm ws}\Delta\Omega \tag{A.9}$$

$$\Delta\dot{\Omega} = k_2 I_{\rm ws}\hat{\mathbf{s}}^T\Delta\boldsymbol{\omega} + k_2\omega_{\rm t} I_{\rm ws}\Delta\gamma \tag{A.10}$$

The characteristic equation of this linear system is

$$\lambda^2(\lambda^3 + a_2\lambda^2 + a_1\lambda + a_0) = 0 \tag{A.11}$$

where

$$a_2 = (1/J_{\rm t})k_2 I_{\rm ws}^2, \quad a_1 = -\frac{k_1 I_{\rm ws}^2 k_2 H_0^2}{J_{\rm t}^2} \quad a_0 = \frac{I_{\rm ws}^2 k_2 H_0^2}{J_{\rm t}^3 J_{\rm a}}(J_{\rm a} - J_{\rm t}).$$

One of the necessary conditions for stability is

$$a_1 > 0$$

which is false for this system. Therefore, this equilibrium is also unstable, and the proof is complete.

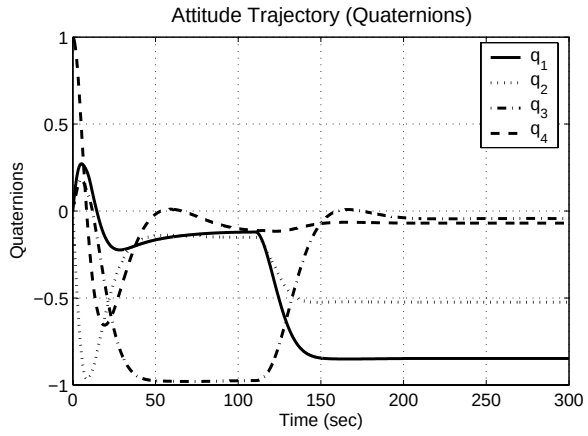


(a) Quaternions (with respect to $\mathcal{I}$).

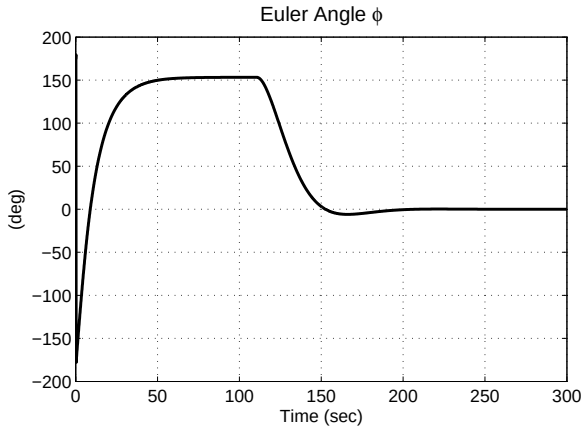


(b) Euler Angle $\phi$ (with respect to $\mathcal{H}$).

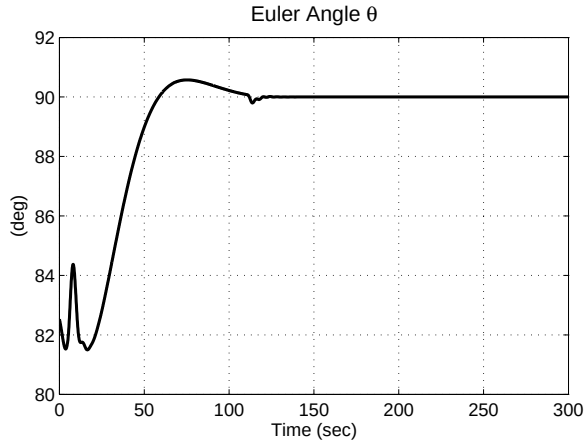


(c) Euler Angle $\theta$ (with respect to $\mathcal{H}$).

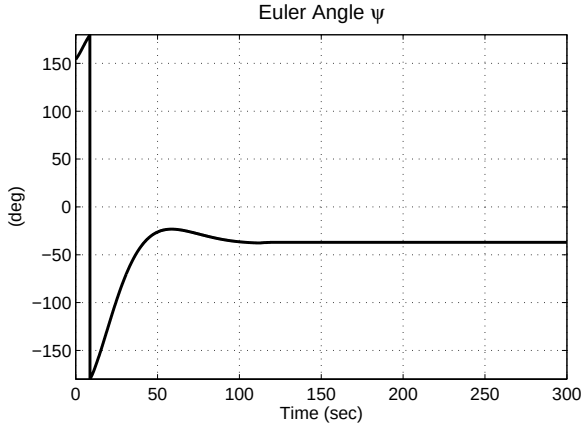


(d) Euler Angle $\psi$ (with respect to $\mathcal{H}$).

**Figure 8. Spacecraft attitude trajectories.**

## Appendix B : Characterization on the Nontrivial Equilibria

In this Appendix, we derive the nontrivial equilibrium states of the closed-loop system under the nonlinear controller (46). These equilibria are characterized by Eq. (48) which is rewritten here as

$$\omega_{\rm t} I_{\rm ws}\Omega - k_\gamma \gamma_e = 0 \quad \text{and} \quad I_{\rm ws}\omega_{\rm s} - k_\Omega \Omega_e = 0. \tag{B.1}$$

We consider two cases: i) $\Omega = 0$ and ii) $\Omega \neq 0$.

i) $\Omega = 0$ : When $\Omega = 0$, then $\Omega_e = -\Omega_{\rm f}^- = H_0/I_{\rm ws}$, and thus $\omega_{\rm s} = k_\Omega H_0/I_{\rm ws}^2$ is a nonzero constant. Rewriting the dynamic equations in the gimbal frame $\mathcal{G}$, one obtains $J\dot{\boldsymbol{\omega}} = -\boldsymbol{\omega}^\times J\boldsymbol{\omega}$, where $\boldsymbol{\omega} = [\omega_{\rm s}, \omega_{\rm t}, \omega_{\rm g}]^T$, $\dot{\boldsymbol{\omega}} = [0, \dot{\omega}_{\rm t}, \dot{\omega}_{\rm g}]^T$. This equation can be written componentwise as

$$\begin{bmatrix} 0 \\ J_{\rm t}\dot{\omega}_{\rm t} \\ J_{\rm a}\dot{\omega}_{\rm g} \end{bmatrix} = \begin{bmatrix} (J_{\rm t} - J_{\rm a})\omega_{\rm t}\omega_{\rm g} \\ -(J_{\rm t} - J_{\rm a})\omega_{\rm g}\omega_{\rm s} \\ 0 \end{bmatrix} \tag{B.2}$$

which immediately yields $\omega_{\rm t}\omega_{\rm g} = 0$ and $\dot{\omega}_{\rm g} = 0$. Moreover, since $\omega_{\rm s}$ and $\omega_{\rm g}$ are constant, $\dot{\omega}_{\rm t}$ is constant, comparing the second element of Eq. (B.2). If $\dot{\omega}_{\rm t}$ is a nonzero constant, $\omega_{\rm t}$ will diverge to infinity thus violating the momentum conservation law. Thus, $\dot{\omega}_{\rm t} = 0$ and $\omega_{\rm g}\omega_{\rm s} = 0$. Since $\omega_{\rm s} = k_\Omega H_0/I_{\rm ws}^2 \neq 0$, it follows that $\omega_{\rm g} = 0$. Therefore, the total angular momentum is

$$\mathbf{h} = [\ J_{\rm t}\frac{k_\Omega H_0}{I_{\rm ws}^2}\ ,\ \ J_{\rm t}\ \omega_{\rm t}\ ,\ \ 0\ ]^T \tag{B.3}$$

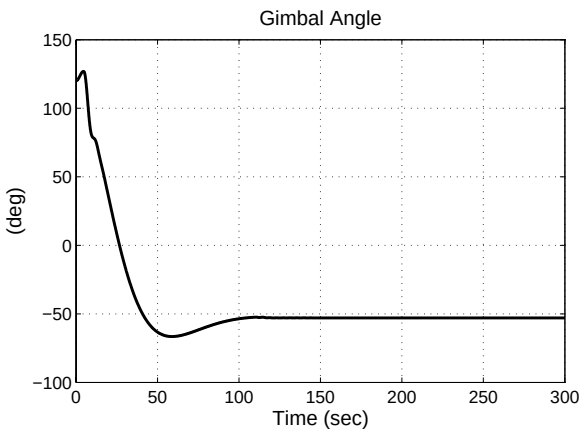


(a) Gimbal angle $\gamma$.

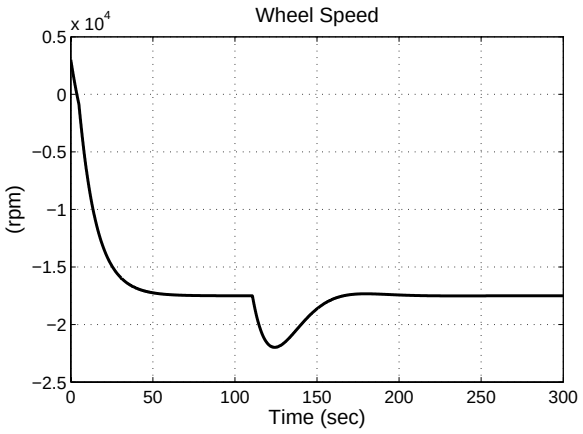


(b) Wheel speed $\Omega$.

**Figure 9. Gimbal angle and wheel speed.**

and thus from $\|\mathbf{h}\| = H_0$, we have that

$$\omega_{\rm t} = \pm\sqrt{\frac{H_0^2}{I_{\rm ws}^4}\left(\frac{I_{\rm ws}^4}{J_{\rm t}^2} - k_\Omega^2\right)}. \tag{B.4}$$

This is the nontrivial equilibrium E1 in Table 1.

ii) $\Omega \neq 0$ : In this case, $\omega_{\rm t}$ is constant, as well as $\omega_{\rm s}$. The equation of motion written in the gimbal frame is

$$J\dot{\boldsymbol{\omega}} = -\boldsymbol{\omega}^\times(J\boldsymbol{\omega} + I_{\rm ws}\Omega\hat{\mathbf{s}}) = -\boldsymbol{\omega}^\times\mathbf{h} \tag{B.5}$$

where

$$\mathbf{h} = [\ J_{\rm t}\omega_{\rm s} + I_{\rm ws}\Omega\ ,\ \ J_{\rm t}\omega_{\rm t}\ ,\ \ J_{\rm a}\omega_{\rm g}\ ]^T \tag{B.6}$$

and $\boldsymbol{\omega} = [\omega_{\rm s}, \omega_{\rm t}, \omega_{\rm g}]^T$, $\dot{\boldsymbol{\omega}} = [0, 0, \dot{\omega}_{\rm g}]^T$. Equivalently,

$$\begin{bmatrix} 0 \\ 0 \\ J_{\rm a}\dot{\omega}_{\rm g} \end{bmatrix} = \begin{bmatrix} \omega_{\rm t}\omega_{\rm g}(J_{\rm t} - J_{\rm a}) \\ \omega_{\rm g}\omega_{\rm s}(J_{\rm a} - J_{\rm t}) - I_{\rm ws}\Omega\omega_{\rm g} \\ I_{\rm ws}\Omega\omega_{\rm t} \end{bmatrix} \tag{B.7}$$

and thus $\omega_{\rm t}\omega_{\rm g} = 0$. Let us consider two cases again: a) $\omega_{\rm g} = 0$ and b) $\omega_{\rm t} = 0$.

ii)-(a) : $\omega_{\rm g} = 0$ : Since $\dot{\omega}_{\rm g} = 0$, $\omega_{\rm t} = 0$ and

$$\mathbf{h} = [J_{\rm t}\omega_{\rm s} + I_{\rm ws}\Omega\ , 0\ ,\ 0\ ]^T = [\ \pm H_0\ ,\ 0\ ,\ 0\ ]^T. \tag{B.8}$$

From Eq. (B.1), $\Omega_e = I_{\rm ws}\omega_{\rm s}/k_\Omega$, and thus $\Omega = \Omega_e + \Omega_{\rm f}^- = I_{\rm ws}\omega_{\rm s}/k_\Omega - H_0/I_{\rm ws}$. Comparing the first element of (B.8) yields

$$\omega_{\rm s}(J_{\rm t} + \frac{I_{\rm ws}^2}{k_\Omega}) = 0, \quad \text{or} \quad \omega_{\rm s}(J_{\rm t} + \frac{I_{\rm ws}^2}{k_\Omega}) = 2H_0. \tag{B.9}$$

If $\omega_{\rm s} = 0$, we are done since this is the desired (trivial) equilibrium. If $\omega_{\rm s} \neq 0$, then

$$\omega_{\rm s} = \frac{2H_0}{J_{\rm t} + I_{\rm ws}^2/k_\Omega}, \tag{B.10}$$

and

$$\Omega = \frac{2I_{\rm ws}H_0}{J_{\rm t}k_\Omega + I_{\rm ws}^2} - \frac{H_0}{I_{\rm ws}}, \tag{B.11}$$

and this state corresponds to the nontrivial equilibrium E2 in Table 1.

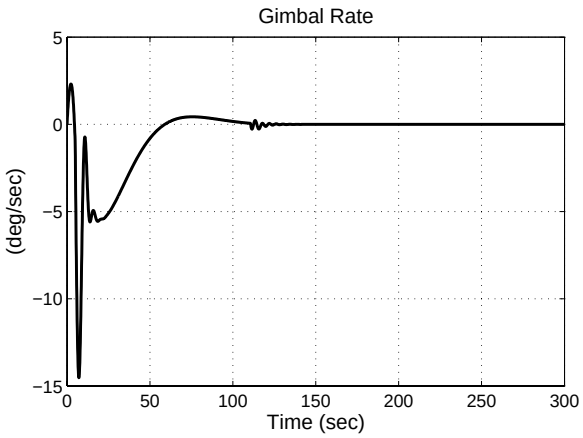


(a) Gimbal rate $\dot{\gamma}$.

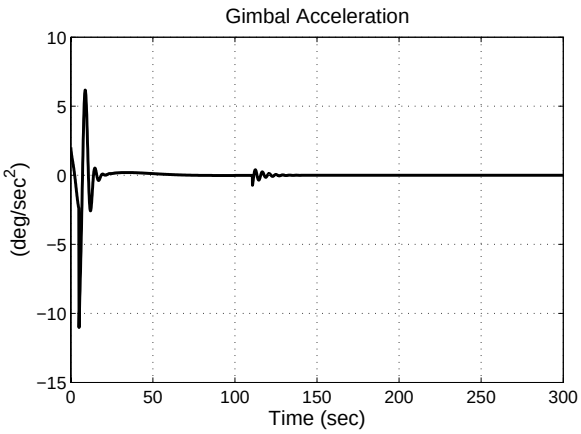


(b) Gimbal acceleration $\ddot{\gamma}$.

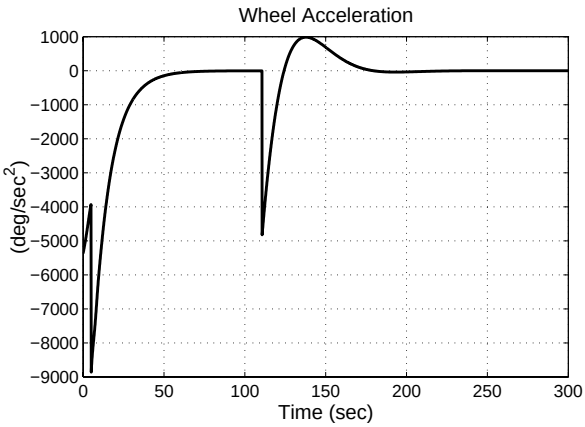


(c) Wheel acceleration $\dot{\Omega}$.

**Figure 10. Control inputs.**

ii)-(b) : $\omega_{\rm t} = 0$ : From Eq. (B.7), $\dot{\omega}_{\rm g} = 0$, thus,

$$\boldsymbol{\omega}^{\times}\mathbf{h} = 0, \tag{B.12}$$

where

$$\boldsymbol{\omega} = [\omega_{\rm s}, 0, \omega_{\rm g}]^T, \quad \mathbf{h} = [J_{\rm t}\omega_{\rm s} + I_{\rm ws}\Omega, 0, J_{\rm a}\omega_{\rm g}]^T. \tag{B.13}$$

Since $\mathbf{h} \neq 0$, this equation implies $\boldsymbol{\omega} = 0$ or $\mathbf{h} = \lambda\boldsymbol{\omega}$ $(\lambda \neq 0)$. The equilibrium with $\boldsymbol{\omega} = 0$ is the desired state, so we can ignore it. From (B.13), therefore, one obtains

$$(J_{\rm t} - \lambda)\omega_{\rm s} = -I_{\rm ws}\Omega \tag{B.14}$$

$$(J_{\rm a} - \lambda)\omega_{\rm g} = 0 \tag{B.15}$$

The case with $\omega_{\rm g} = 0$ has been examined already, so we only need to check the case $\lambda = J_{\rm a}$. For this case, it is easy to show that

$$\omega_{\rm s} = \frac{-H_0}{J_{\rm a} - J_{\rm t} - I_{\rm ws}^2/k_\Omega}, \tag{B.16}$$

$$\omega_{\rm g} = \pm\sqrt{H_0^2\left(\frac{1}{J_{\rm a}^2} - \frac{1}{(J_{\rm a} - J_{\rm t} - I_{\rm ws}^2/k_\Omega)^2}\right)}, \tag{B.17}$$

where we have used the fact that $\Omega = \Omega_e + \Omega_{\rm f}^- = \frac{I_{\rm ws}\omega_{\rm s}}{k_\Omega} - \frac{H_0}{I_{\rm ws}}$ and $\|\mathbf{h}\| = H_0$. These equilibrium states correspond to E3 in Table 1.

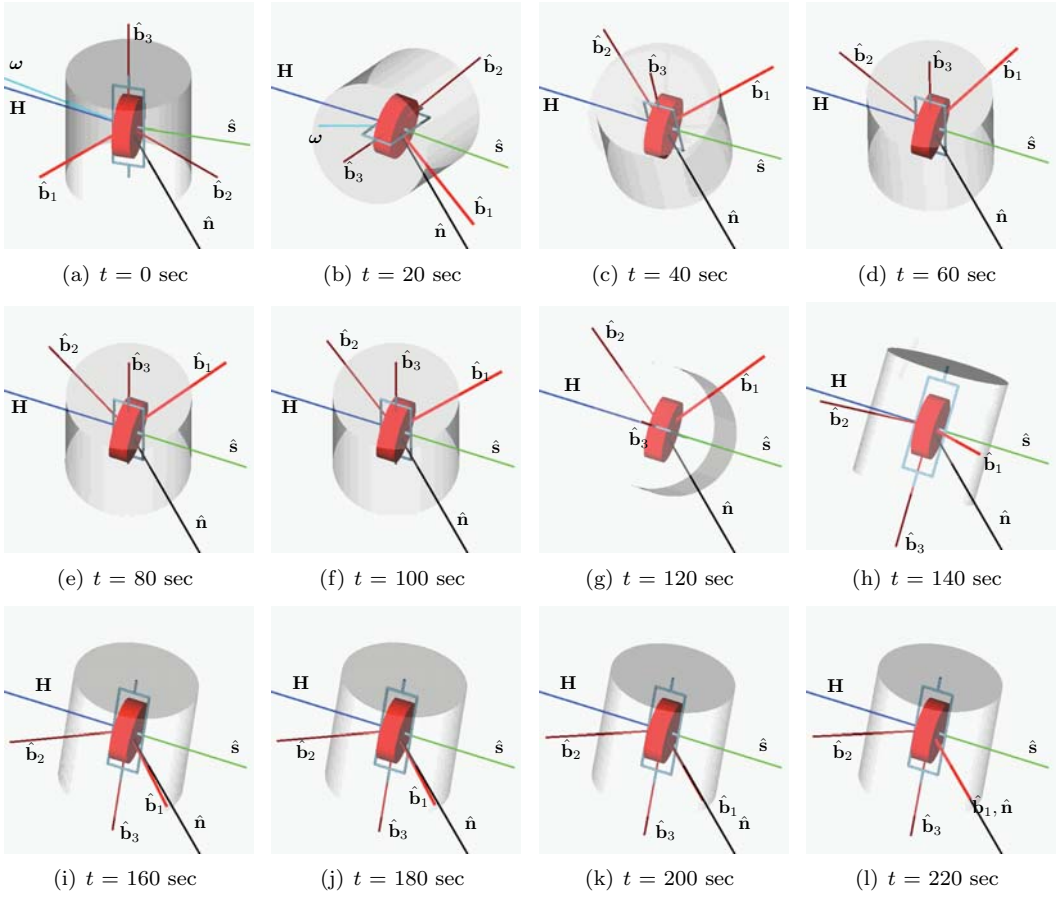


(a) $t = 0$ sec (b) $t = 20$ sec (c) $t = 40$ sec (d) $t = 60$ sec

(e) $t = 80$ sec (f) $t = 100$ sec (g) $t = 120$ sec (h) $t = 140$ sec

(i) $t = 160$ sec (j) $t = 180$ sec (k) $t = 200$ sec (l) $t = 220$ sec

**Figure 11. Snapshots of the spacecraft orientation during the maneuver.**

# References


[1]Vadali, S. R., "Variable-Structure Control of Spacecraft Large-Angle Maneuvers," *Journal of Guidance, Control, and Dynamics*, Vol. 9, No. 2, 1989, pp. 235–239.

[2]Sheen, J. J. and Bishop, R. H., "Spacecraft Nonlinear Control," *AIAA/AAS Astrodynamics Conference*, Hilton Head, SC, Aug. 10-12, 1992, Paper AAS 92-172.

[3]Wen, J. T. and Kreutz-Delgado, K., "The attitude control problem," *IEEE Transactions on Automatic Control*, Vol. 36, No. 10, 1991, pp. 1148–1162.

[4]Ahmed, J., Coppola, V., and Bernstein, D. S., "Adaptive Asymptotic Tracking of Spacecraft Attitude Motion with Inertia Matrix Identification," *Journal of Guidance, Control, and Dynamics*, Vol. 21, No. 5, 1998, pp. 684–691.

[5]Schaub, H., Akella, M. R., and Junkins, J. L., "Adaptive Control of Nonlinear Attitude Motions Realizing Linear Closed-Loop Dynamics," *Proceedings of the American Control Conference*, 1999, pp. 1563–1567, San Diego, CA.

[6]Junkins, J. L. and Turner, J., *Optimal Spacecraft Rotational Maneuvers*, Elsevier, New York, 1986.

[7]Shen, H. and Tsiotras, P., "Time-Optimal Control of Axi-symmetric Spacecraft," *Journal of Guidance, Control, and Dynamics*, Vol. 22, No. 5, 1999, pp. 682–694.

[8]Osipchuk, M., Bharadwaj, S., and Mease, K., "Achieving Good Performance in Global Attitude Stabilization," *Proceedings of the American Control Conference*, 1997, pp. 403–407, Albuquerque, NM.

[9]Singh, S. A., "Robust Nonlinear Attitude Control of Flexible Spacecraft," *IEEE Transactions on Aerospace and Electronic Systems*, Vol. 23, No. 2, 1987, pp. 380–387.

[10]Lintereur, B. V. and McGovern, L. K., "Constrained $\mathcal{H}_2$ Design via Convex Optimization Applied to Precision Pointing Attitude Control," *Proc. of the 36th IEEE Conference on Decision and Control*, 1997, pp. 1300–1304, San Diego, CA.

[11]Boskŏvić, J. D., Li, S.-M., and Mehra, R. K., "Robust stabilization of spacecraft in the presence of control input saturation using sliding mode control," *AIAA Guidance, Navigation, and Control Conference*, 1999, pp. 1960–1970, Portland, OR.

[12]Aeyels, D. and Szafranski, M., "Comments on the stabilizability of the angular velocity of a rigid body," *Systems and Control Letters*, Vol. 10, No. 1, 1988, pp. 35–39.

[13]Sontag, E. and Sussmann, H., "Further comments on the stabilizability of the angular velocity of a rigid body," *Systems and Control Letters*, Vol. 12, No. 3, 1988, pp. 213–217.

[14]Andriano, V., "Global Feedback Stabilization of the Angular Velocity of a Symmetric Rigid Body," *Systems and Control Letters*, Vol. 20, 1993, pp. 361–364.

[15]Morin, P., "Robust Stabilization of the Angular Velocity of a Rigid Body with Two Controls," *European Journal of Control*, Vol. 1, 1996, pp. 51–56.

[16]Tsiotras, P. and Schleicher, A., "Detumbling and Partial Attitude Stabilization of a Rigid Spacecraft Under Actuator Failure," *AIAA Guidance, Navigation and Control Conference*, Denver, CO, 2000, AIAA Paper 00-4044.

[17]Byrnes, C. I. and Isidori, A., "On the attitude stabilization of a rigid spacecraft," *Automatica*, Vol. 27, No. 1, 1991, pp. 87–95.

[18]Krishnan, H., Reyhanoglu, M., and McClamroch, H., "Attitude stabilization of a rigid spacecraft using two control torques: A nonlinear control approach based on the spacecraft attitude dynamics," *Automatica*, Vol. 30, No. 6, 1994, pp. 1023–1027.

[19]Tsiotras, P., Corless, M., and Longuski, M., "A Novel Approach to the Attitude Control of Axisymmetric Spacecraft," *Automatica*, Vol. 31, No. 8, 1995, pp. 1099–1112.

[20]Coron, J. M. and Keraï, E. L., "Explicit Feedback Stabilizing the Attitude of a Rigid Spacecraft with Two Control Torques," *Automatica*, Vol. 32, No. 5, 1996, pp. 669–677.

[21]Morin, P. and Samson, C., "Time-Varying Exponential Stabilization of a Rigid Spacecraft with Two Control Torques," *IEEE Transactions on Automatic Control*, Vol. 42, No. 4, 1997, pp. 528–534.

[22]Spindler, K., "Attitude Control of Underactuated Spacecraft," *European Journal of Control*, Vol. 6, No. 3, 2000, pp. 229–242.

[23]Tsiotras, P. and Luo, J., "Stabilization and Tracking of Underactuated Axi-symmetric Spacecraft with Bounded Inputs," *Automatica*, Vol. 36, No. 8, 2000, pp. 1153–1169.

[24]Tsiotras, P. and Doumtchenko, V., "Control of Spacecraft Subject to Actuator Failures: State-of-the-Art and Open Problems," *Proceedings of the R.H. Battin Astrodynamics Symposium*, College Station, TX, March 20-21, 2000, AAS Paper 00-264.

[25]Krishnan, H., McClamroch, H., and Reyhanoglu, M., "Attitude Stabilization of a Rigid Spacecraft Using Two Momentum Wheel Actuators," *Journal of Guidance, Control, and Dynamics*, Vol. 18, No. 2, 1995, pp. 256–263.

[26]Kim, S. and Kim, Y., "Spin-Axis Stabilization of a Rigid Spacecraft Using Two Reaction Wheels," *Journal of Guidance, Control, and Dynamics*, Vol. 24, No. 5, 2001, pp. 321–331.

[27]Vadali, S. R. and Junkins, J. L., "Spacecraft Large Angle Rotational Maneuvers with Optimal Momentum Transfer," *Journal of the Astronautical Sciences*, Vol. 31, No. 2, 1983, pp. 2178–235.

[28]Hall, C., "Momentum Transfer in Two-Rotor Gyrostats," *Journal of Guidance, Control, and Dynamics*, Vol. 19, No. 5, 1996, pp. 1157–1161.

[29]Bang, H., Myung, H.-S., and Tahk, M.-J., "Nonlinear Momentum Transfer Control of Spacecraft by Feedback Linearization," *Journal of Spacecraft and Rockets*, Vol. 39, No. 6, 2002, pp. 866–873.

[30]Ford, K. A. and Hall, C. D., "Flexible Spacecraft Reorientations Using Gimbaled Momentum Wheels," *Advances in the Astronautical Sciences, Astrodynamics*, edited by F. Hoots, B. Kaufman, P. J. Cefola, and D. B. Spencer, Vol. 97, Univelt, San Diego, 1997, pp. 1895–1914.

[31]Schaub, H., Vadali, S. R., and Junkins, J. L., "Feedback Control Law for Variable Speed Control Moment Gyroscopes," *Journal of the Astronautical Sciences*, Vol. 46, No. 3, 1998, pp. 307–328.

[32]Schaub, H. and Junkins, J. L., "Singularity Avoidance Using Null Motion and Variable-Speed Control Moment Gyros," *Journal of Guidance Control, and Dynamics*, Vol. 23, No. 1, 2000, pp. 11–16.

[33]Yoon, H. and Tsiotras, P., "Spacecraft Adaptive Attitude And Power Tracking With Variable Speed Control Moment Gyroscopes," *Journal of Guidance, Control, and Dynamics*, Vol. 25, No. 6, Nov.-Dec. 2002, pp. 1081–1090.

[34]Yoon, H. and Tsiotras, P., "Singularity Analysis of Variable-Speed Control Moment Gyros," *Jornal of Guidance, Control, and Dynamics*, Vol. 27, No. 3, 2004, pp. 374–386.

[35]Marshall, A. and Tsiotras, P., "Spacecraft Angular Velocity Stabilization Using A Single-Gimbal Variable Speed Control Moment Gyro," *AIAA Guidance, Navigation and Control Conference*, Austin, TX, 2003, AIAA Paper 03-5654.

[36]Richie, D. J., Tsiotras, P., and Fausz, J. L., "Simultaneous Attitude Control and Energy Storage using VSCMGs : Theory and Simulation," *Proceedings of American Control Conference*, 2001, pp. 3973–3979.

[37]Kailath, T., *Linear Systems*, Prentice-Hall, Englewood Cliffs, New Jersey, 1980, pp. 135–139.

[38]Tsiotras, P., Yoon, H., and Marshall, A., "Controllability Analysis and Control of Spacecraft Using A Single-Gimbal Variable-Speed Control Moment Gyroscope," Internal Report, School of Aerospace Engineering, Georgia Institute of Technology, Atlanta, GA, January 2004.

[39]Brogan, W. L., *Modern Control Theory*, Prentice Hall, New Jersey, 3rd ed., 1991, pp. 515–523.